TTI: 0-6889

Texas A&M Transportation Institute

Evaluation of the Rolling Density Meter for Rapid Continuous Measurement of Asphalt Mixture Density

Technical Report 0-6889-R1

Cooperative Research Program

TEXAS A&M TRANSPORTATION INSTITUTE
COLLEGE STATION, TEXAS

in cooperation with the
Federal Highway Administration and the
Texas Department of Transportation
http://tti.tamu.edu/documents/0-6889-R1.pdf

Technical Report Documentation Page

1. Report No.	2. Government Accession No.	3. Recipient's Catalog No.
FHWA/TX-17/0-6889-R1		

4. Title and Subtitle	5. Report Date
EVALUATION OF THE ROLLING DENSITY METER FOR RAPID CONTINUOUS MEASUREMENT OF ASPHALT MIXTURE DENSITY	Published: January 2019
	6. Performing Organization Code

7. Author(s)	8. Performing Organization Report No.
Bryan Wilson, Stephen Sebesta, and Tom Scullion	Report 0-6889-R1

9. Performing Organization Name and Address	10. Work Unit No. (TRAIS)
Texas A&M Transportation Institute College Station, Texas 77843-3135	
	11. Contract or Grant No. Project 0-6889

12. Sponsoring Agency Name and Address	13. Type of Report and Period Covered
Texas Department of Transportation Research and Technology Implementation Office 125 E. 11th Street Austin, Texas 78701-2483	Technical Report: January 2016–December 2017
	14. Sponsoring Agency Code

15. Supplementary Notes

Project performed in cooperation with the Texas Department of Transportation and the Federal Highway Administration.
Project Title: Rolling Density Meter to Ensure Long Term Performance of Flexible Pavements
URL: http://tti.tamu.edu/documents/0-6889-R1.pdf

16. Abstract

The rolling-density meter (RDM) is a ground-penetrating radar (GPR)-based system tailored for rapidly and continuously measuring asphalt mixture density. This research analyzed the readiness level of the RDM and provided recommendations for how this technology could be used in QC/QA.

To evaluate the RDM precision, four antennas were used in a laboratory environment to test six different materials. Increasing the number of scans averaged did improve the precision. For materials similar to those tested, the dielectric measurement was repeatable within 0.15 and reproducible within 0.22 or better.

The RDM was deployed on six field projects for multiple paving days. Researchers evaluated the reproducibility of calibration curves, precision and bias of the system and of a nuclear density gage, and distribution of predicted air voids. Overall air void calibrations were good with an average R^2 value of 0.76. The calibration curves were unique for different paving projects, and in some cases unique for different days of paving. Using different antennas for calibration did not influence the resulting calibration curves. The RDM was more precise than the nuclear density gauge and unbiased.

The field data were used to perform a producer and consumer risk analysis. Different pay factors and percent within limit characterizations were calculated. The single-core acceptance method exposes producers and consumers to significant risk while density profiling with the RDM effectively eliminates risk.

An alternative 3D radar system was deployed on three test sections. The system produced high resolution scans of the asphalt surface and subsurface. Further work is needed to tailor data processing for density testing.

Researchers recommend adopting the draft test method and equipment specifications for rapid full-coverage measurements of asphalt mixture density using GPR.

17. Key Words	18. Distribution Statement
Quality Control, Quality Assurance, Density, Air voids, Dielectric Constant, GPR, Rolling density meter, Asphalt Mixture	No restrictions. This document is available to the public through NTIS: National Technical Information Service Alexandria, Virginia http://www.ntis.gov

19. Security Classif. (of this report)	20. Security Classif. (of this page)	21. No. of Pages	22. Price
Unclassified	Unclassified	94	

Form DOT F 1700.7 (8-72) Reproduction of completed page authorized

EVALUATION OF THE ROLLING DENSITY METER FOR RAPID CONTINUOUS MEASUREMENT OF ASPHALT MIXTURE DENSITY

by

Bryan Wilson
Associate Research Scientist
Texas A&M Transportation Institute

Stephen Sebesta
Research Scientist
Texas A&M Transportation Institute

and

Tom Scullion
Senior Research Engineer
Texas A&M Transportation Institute

Report 0-6889-R1
Project 0-6889
Project Title: Rolling Density Meter to Ensure Long Term Performance of Flexible Pavements

Performed in cooperation with the
Texas Department of Transportation
and the
Federal Highway Administration

Published: January 2019

TEXAS A&M TRANSPORTATION INSTITUTE
College Station, Texas 77843-3135

DISCLAIMER

This research was performed in cooperation with the Texas Department of Transportation (TxDOT) and the Federal Highway Administration (FHWA). The contents of this report reflect the views of the authors, who are responsible for the facts and the accuracy of the data presented herein. The contents do not necessarily reflect the official view or policies of the FHWA or TxDOT. This report does not constitute a standard, specification, or regulation.

ACKNOWLEDGMENTS

This project was conducted in cooperation with TxDOT and FHWA. The authors thank the TxDOT Project Manager Joe Adams, and members of the TxDOT project team: Brett Haggerty, Johnny Johnson, and Robert Lee.

Field evaluations were coordinated and constructed with the help of Stephen Kasberg (TxDOT-Waco), Sarah Horner (TxDOT-Waco), James Robbins (TxDOT-Bryan), Connie Flickinger (TxDOT-Bryan), Big Creek Construction, Knife River Construction, and Lone Star Paving. Geophysical survey systems (GSSI) provided ongoing technical and product support for the equipment. TTI personal assisted with field and laboratory testing, namely Tyler Gustavus, Rick Canatella, Tony Barbosa, Soohyok Im, Tommy Blackmore, and Ross Taylor. The following Texas A&M students also participated in testing: Ashlesh Kurahatti, Purvit Soni, and Saatvik Satyaprakash.

TABLE OF CONTENTS

Page

LIST OF FIGURES

Page

LIST OF TABLES

Page

CHAPTER 1—INTRODUCTION

PROBLEM STATEMENT

Compaction is a key component in constructing asphalt pavements with good performance. Insufficient compaction can result in premature permanent deformation, excessive aging, and moisture damage even if all other mixture design characteristics are met (*1*). Currently, the Texas Department of Transportation (TxDOT) measures the roadway compaction of asphalt mixtures through field coring where one pair of cores is collected per sublot. This low level of testing coverage results in high producer and consumer risks, posing good chances for missing localized problem areas that govern the life of the pavement.

The GSSI Rolling Density Meter (RDM) is a ground penetrating radar (GPR) system, tailored for asphalt mixture density testing (Figure 1). Recent pilot work has shown its promise to rapidly scan and measure surface layer density at 6-in. intervals (*2*). The ability to supplement, and possibly eventually replace, most field coring activities for acceptance offers several advantages to stakeholders:

- Large areas can be quickly tested with minimal disruption to traffic.
- Exposure of workers in the right of way may be reduced.
- Longitudinal joint density can be evaluated for specification compliance.
- Extensive testing coverage would reduce producer and consumer risks.

Figure 1. RDM.
(3-channel system. 1-channel system also available.)

The driving force behind this technology is that an improved density test method would encourage improved compaction practices. This, in turn, would foster longer lasting pavements with reduced life cycle costs.

OBJECTIVES AND SCOPE

The research objective was to analyze the readiness level of the RDM and provide recommendations for how this technology could be used in quality control/quality assurance (QC/QA). The system and methods would need to be technically sound and testing limitations clearly defined. Ideally the hardware would be robust, the software user-friendly, and the testing minimally intrusive to the current construction work flow.

The scope of this research was:

- Develop RDM precision estimates in a laboratory environment.
- Deploy the RDM in the field on six paving projects for three days of paving each:
    - Evaluate reproducibility of calibration curves considering different antennas and variation in daily mixture production.
    - Measure the precision and bias of the system and calibration methods.
    - Assess the air void content distributions of the constructed mat.
    - Conduct a producer and consumer risk analysis.
- Evaluate an alternative 3D radar system.
- Develop draft test methods and specifications.
- Conduct a webinar presenting findings and recommended future directions.

CHAPTER 2—BACKGROUND

GROUND-PENETRATING RADAR

GRP has shown significant promise as a rapid, continuous test method for QC/QA of in-field density in several past research studies (*2, 3, 4, 5, 6, 7*). GPR works by sending discrete pulses of electromagnetic waves into the pavement and capturing the reflections as the signal moves between different layers. The amplitude of radar reflections and the time delay between reflections are used to calculate layer dielectrics (Equation 1). Figure 2 shows dielectrics for various materials. Within a given pavement layer, as the dielectric approaches 1.0, the air void content is assumed to increase. General surface dielectric values for hot mix asphalt (HMA) are between 4 and 6, depending on the aggregate type, asphalt content, and gradation. Very high dielectric values often indicate moisture on the surface.

$$\sqrt{\varepsilon_p} = \frac{1 - \frac{A_p}{A_m}}{1 + \frac{A_p}{A_m}} \qquad \text{(Equation 1)}$$

Where:

ε_p = Dielectric value of the pavement surface.
A_p = Reflection amplitude from the pavement surface.
A_m = Source amplitude, as estimated with a metal plate reflection measurement.

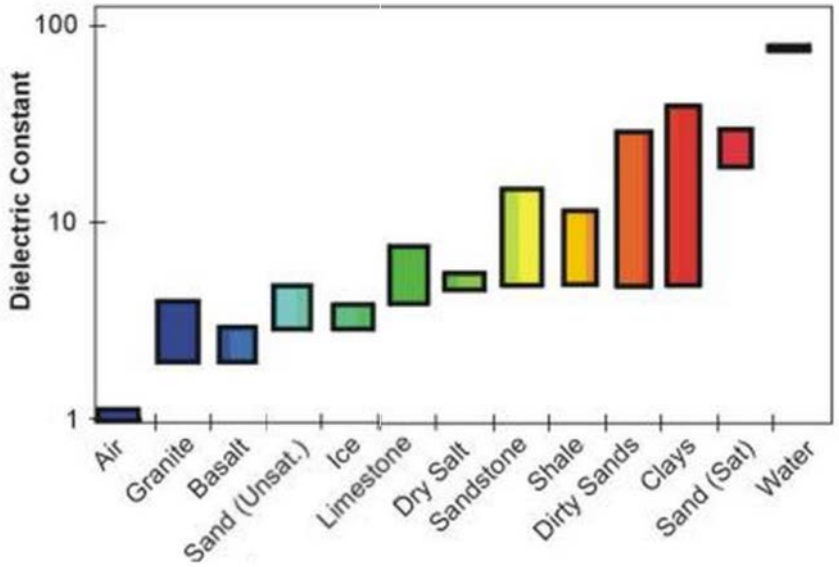

Figure 2. Materials and Associated Dielectric Constants (*8*).

Lower frequency radar can penetrate deep into the pavement, while higher frequency radar (2 GHz and greater) will measure shallower depths at a higher resolution. A high-frequency radar, therefore, could have good resolution for typical HMA overlays less than 2 in. thick. Another advantage with a smaller, high-frequency antenna is that the unit is more portable, and

easier to deploy for quick, nondestructive field measurements. The greatest benefit of the system, however, is the ability to collect continuous measurements rapidly.

METHODS OF HMA AIR VOID PREDICTION FROM DIELECTRIC

There are two general methods, both well represented in the literature, used to predict the HMA air void content from dielectric measurements:

1. Empirical calibrations between sampled core voids and the HMA dielectric constant (*2, 3, 9, 10, 11, 12*).

2. Micro-mechanics modeling of the composite dielectric based on mixture composition (*13, 14, 15, 16, 17*).

Both approaches produced reliable results. The empirical approach is intuitive and can be performed with basic non-linear regression analysis. The draw-back is that every mix design requires a new calibration, which can take 24 hours to establish. Also, the original calibration may become invalid if the design changes over the course of construction. The micro-mechanics model is also relatively intuitive, even though the calculations appear more complicated. With this method, mixture details can be measured beforehand and input into the model before construction even starts. The mixture details can also be adjusted as the mix design changes. This research focuses on the precision and bias of the empirical calibration approach. Future research should address the micro-mechanics approach.

PRECISION AND BIAS

Precision and bias of measurements are a critical aspect of any test method. The precision and bias help define how a user might interpret a set of results for decision making. In general, the better the precision and bias of test method, the more useful the test will be. The American Society for Testing and Materials (ASTM) provides guidance on the precision, bias, and other related statistics as defined in ASTM E177 (Standard Practice for Use of the Terms Precision and Bias in ASTM Test Methods). Precision and bias are defined as follows:

- Precision: The degree of agreement within a set of observations or test results.
- Bias: The difference between expected test results and the true value or reference value. It is the total systematic error as contrasted to random error.
- Accuracy: The degree of agreement between a test value and the true value or reference value. It encompasses both the systematic and random error.

Repeatability and reproducibility are subcategories of precision.

- Repeatability: The precision when performing multiple measurements of given items under identical test conditions (i.e., same operator, same equipment, same lab, within short time intervals).
- Reproducibility: The precision when performing measurements of given items under different test conditions (i.e., different operator, different equipment, different lab, and different times).

PRODUCER AND CONSUMER RISK

In asphalt construction, risk to the agency (consumer risk) is when the agency accepts or rejects a whole day's production based on the results of a few random sample locations. In the end, the actual compaction variability on a project is unknown. In the scenario in Figure 3a, the agency would accept the production based on the spot measurement, while the actual project has significant areas of under-compaction (a statistical Type II error). Since the life of a pavement is often governed by the worst-performing locations, the agency mistakenly accepts construction with limited life.

On the other hand, risk to the contractor (producer risk) occurs when the random sample location coincides with localized under-compacted areas (Figure 3b). In this case, the contractor receives a penalty for the day's production despite the fact that the large majority of the construction was acceptable (a statistical Type I error).

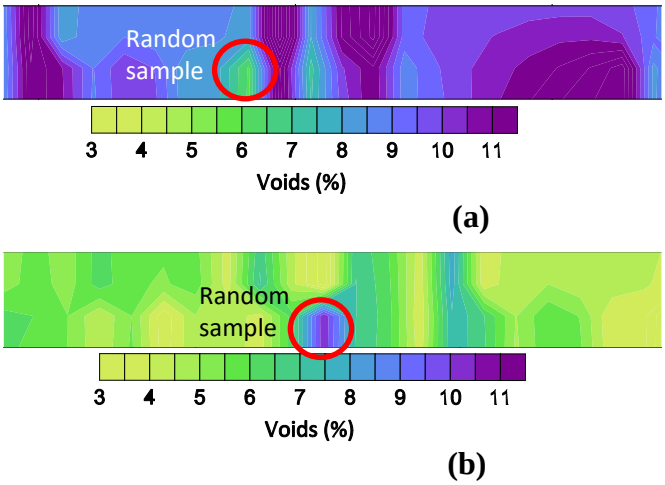

Type II Error
Accepting production that should be rejected.

Type I Error
Rejecting production that should be accepted.

Figure 3. Examples of a) Consumer Risk and b) Producer Risk.

CHAPTER 3—LABORATORY PRECISION ANALYSIS

OVERVIEW

To evaluate the RDM precision, four different antennas were evaluated in a laboratory environment on six different materials. This chapter first presents test procedures, followed by the results and conclusion.

PROCEDURES

Researchers identified, sampled, and fabricated test slabs for precision testing using a thin overlay mix (TOM) and a Type C (TY C) mix. Researchers fabricated three slabs with each mix at different densities to meet the minimum of six materials required for development of precision estimates.

Researchers developed and set up a system to precisely align the RDM repeatedly over the same spot of the asphalt mixture slabs to minimize variability from system positioning. Four different GPR antennas were used in the analysis. With each antenna and test slab, researchers collected measurements as follows to represent different expected test conditions:

- Constant on: 10 tests evenly spaced over a 1-hour period to represent the time frame for conducting a typical field survey.
- Hard reset: 10 tests after hard reset with at least 1 hour of system shut down, to represent shutting down the system and returning to the survey site for additional testing at a later time.

Researchers collected at least 1,000 scans in the time mode for each test. In reducing each data file, staff reported the dielectric from each test with two different approaches to represent the minimum and maximum number of scans that may be suitable for averaging depending on the forward travel speed of the radar system when used in the field:

- Average 5 scans starting with scan number 200.
- Average 500 scans starting with scan number 200.

With the data reduced, researchers analyzed the data as follows:

- Used a paired t-test to evaluate if the average dielectric from five scans is equivalent to the average value from 500 scans.
- Used processing methods of ASTM E691 to develop repeatability and reproducibility estimates for the measured dielectric values.

Figure 4 shows the general test arrangement. The antennas were operated at a distance of 11.5 in. from the asphalt surface to the bottom of the antenna. The antennas were leveled within ±0.0° on the transverse axis and within ±0.5° on the longitudinal axis. An alignment method was used to position each antenna at the same location over each test slab within ±0.15 in. The ambient environment during testing was 22 ±2°C.

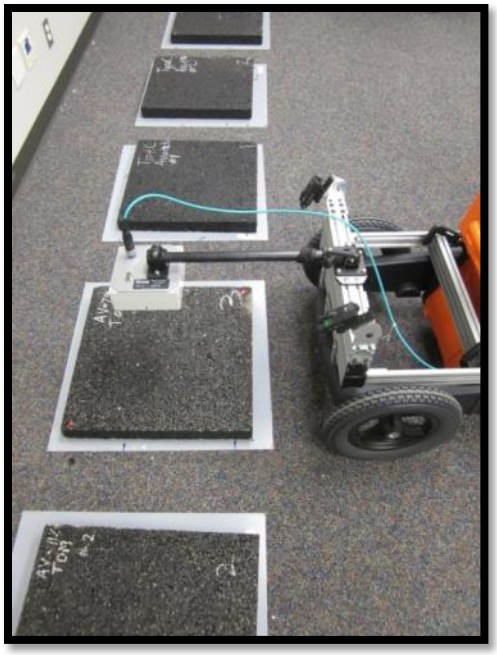

Figure 4. Test Arrangement for Precision of Radar System.

Researchers also investigated the impact of layer thickness on the GPR measurements. Researchers used the precision data to perform an analytical study on the impact of how GPR reproducibility may impact calibration needs.

RESULTS

Table 1 presents the paired t-test results. Using a 5 percent level of significance, the results show:

- For a given antenna and test condition, only Antenna 7A resulted in computed dielectrics that differed according to how many scans were averaged.
- For all antennas pooled within a test condition, the number of scans averaged did not influence the computed dielectric for the constant on condition. For all antennas pooled with the hard reset test condition, the number of scans averaged did produce statistically different results.
- For all antennas and test conditions pooled, the number of scans averaged did produce statistically different results.

Further investigation of these data in Table 1 revealed that, if Antenna 7A is omitted, the computed dielectric value is not impacted by whether five scans or 500 scans are averaged to report the test result.

Table 1. Paired t-Test Results for Computing Dielectric with Either 5 or 500 Scans.

Test Condition	Antenna	Slab	xbar 5	xbar 500	Difference	p value (1 antenna)	p value (test condition) (all antenna,	p value (all)
Constant On	8	1	6.4234	6.4199	-0.0035	0.768	0.242	0.016
		2	5.9556	5.9566	0.0010			
		3	6.0472	6.0351	-0.0121			
		4	4.9851	4.9915	0.0064			
		5	5.1274	5.1380	0.0106			
		6	4.3705	4.3742	0.0037			
	7a	1	6.6090	6.5835	-0.0256	0.032		
		2	6.1173	6.1236	0.0062			
		3	6.0623	6.0097	-0.0526			
		4	5.0410	4.9865	-0.0544			
		5	4.9896	4.9740	-0.0156			
		6	4.3537	4.3293	-0.0244			
	7b	1	6.3070	6.3156	0.0085	0.228		
		2	6.1051	6.1221	0.0170			
		3	5.9476	5.9537	0.0061			
		4	5.0333	5.0351	0.0018			
		5	5.0276	5.0150	-0.0126			
		6	4.3401	4.3554	0.0153			
	3	1	6.4114	6.4017	-0.0097	0.573		
		2	6.0403	6.0550	0.0147			
		3	6.0007	6.0068	0.0062			
		4	5.0652	5.0671	0.0018			
		5	5.0983	5.0937	-0.0046			
		6	4.4239	4.4281	0.0042			
Hard Reset	8	1	6.4647	6.4516	-0.0131	0.592	0.010	
		2	6.0623	6.0507	-0.0116			
		3	6.0257	6.0419	0.0162			
		4	5.0198	5.0119	-0.0079			
		5	5.1043	5.0969	-0.0074			
		6	4.4048	4.4121	0.0073			
	7a	1	6.6744	6.6540	-0.0203	0.002		
		2	6.2088	6.1817	-0.0270			
		3	6.1864	6.1654	-0.0210			
		4	5.0333	5.0173	-0.0160			
		5	5.0733	5.0630	-0.0104			
		6	4.3804	4.3714	-0.0091			
	7b	1	6.4687	6.4785	0.0098	0.582		
		2	6.0827	6.0837	0.0010			
		3	6.0523	6.0539	0.0016			
		4	5.0509	5.0316	-0.0194			
		5	5.0724	5.0731	0.0007			
		6	4.3783	4.3701	-0.0082			
	3	1	6.4769	6.4605	-0.0164	0.464		
		2	6.0756	6.0592	-0.0164			
		3	6.0400	6.0308	-0.0092			
		4	4.9890	5.0022	0.0132			
		5	5.0529	5.0562	0.0032			
		6	4.3664	4.3685	0.0022			

Due to the observed potential influence of the number of scans averaged, researchers developed precision statistics for each test condition both by averaging five scans and by averaging 500 scans. Figure 5 illustrates the repeatability limits.

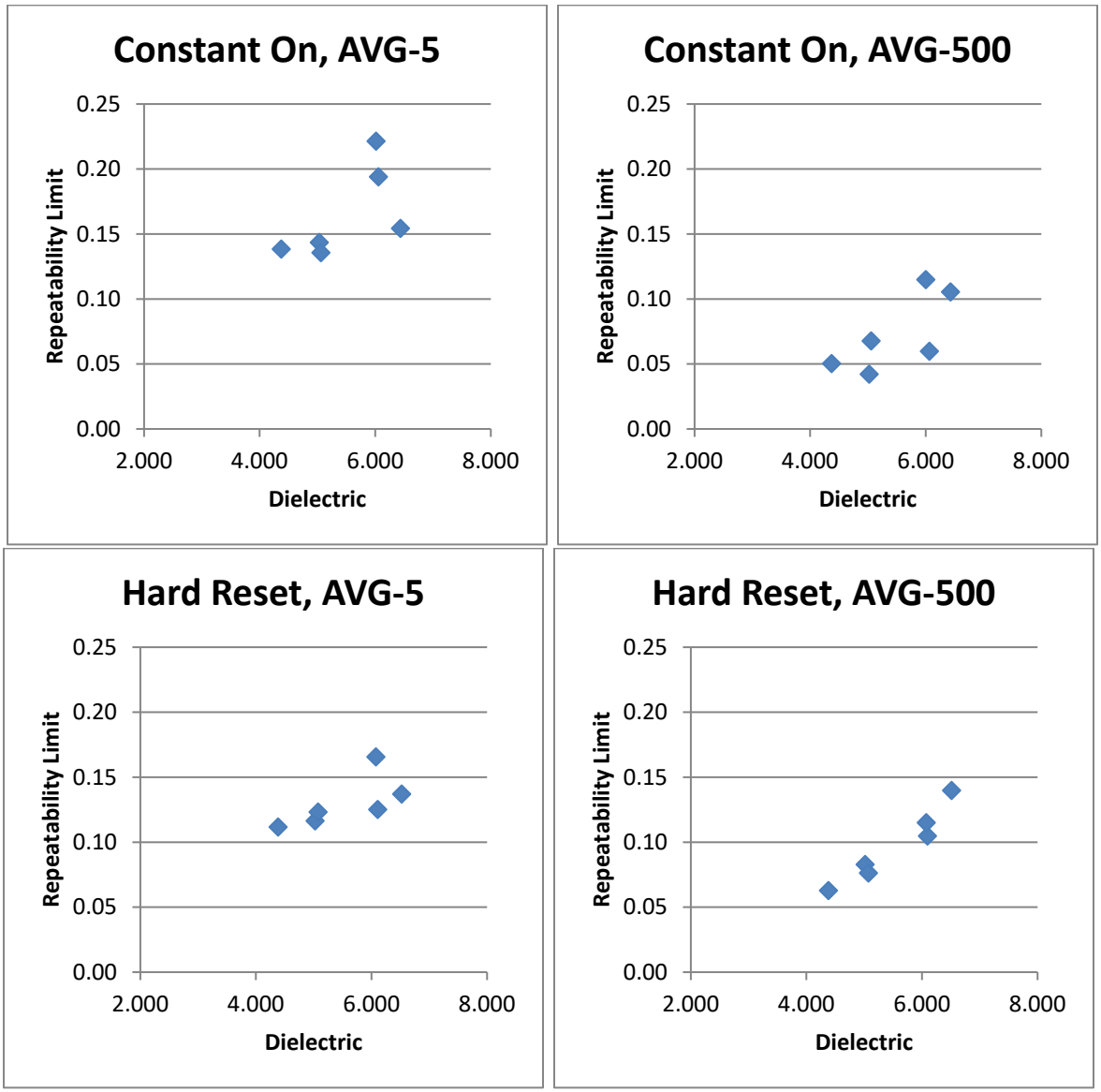

Figure 5. Summary Repeatability Limits by Test Condition and Number of Scans Averaged.

The results in Figure 5 illustrate that:

- The dielectric values included in the precision tests ranged from 4.4 to 6.4.
- Within that range of dielectric values:
    - The repeatability limit averaged 0.15 when using five scans to generate a measurement, and the repeatability limit averaged 0.09 when using 500 scans to generate a measurement.
    - With some test conditions and data processing methods, the precision limit may increase as the actual material dielectric constant increases. This situation of increased variability with increasing level is common with many tests and not a cause for concern. The data show the overall repeatability coefficient of variation is about 0.8 percent, and the overall reproducibility coefficient of variation is about 1.25 percent.

For the influence of layer thickness, Figure 6 shows that the RDM can test down to a surface layer thickness of about 0.75 in. without interference from the layer below. This thickness should prove suitable for all but the thinnest of overlays currently in use within TxDOT.

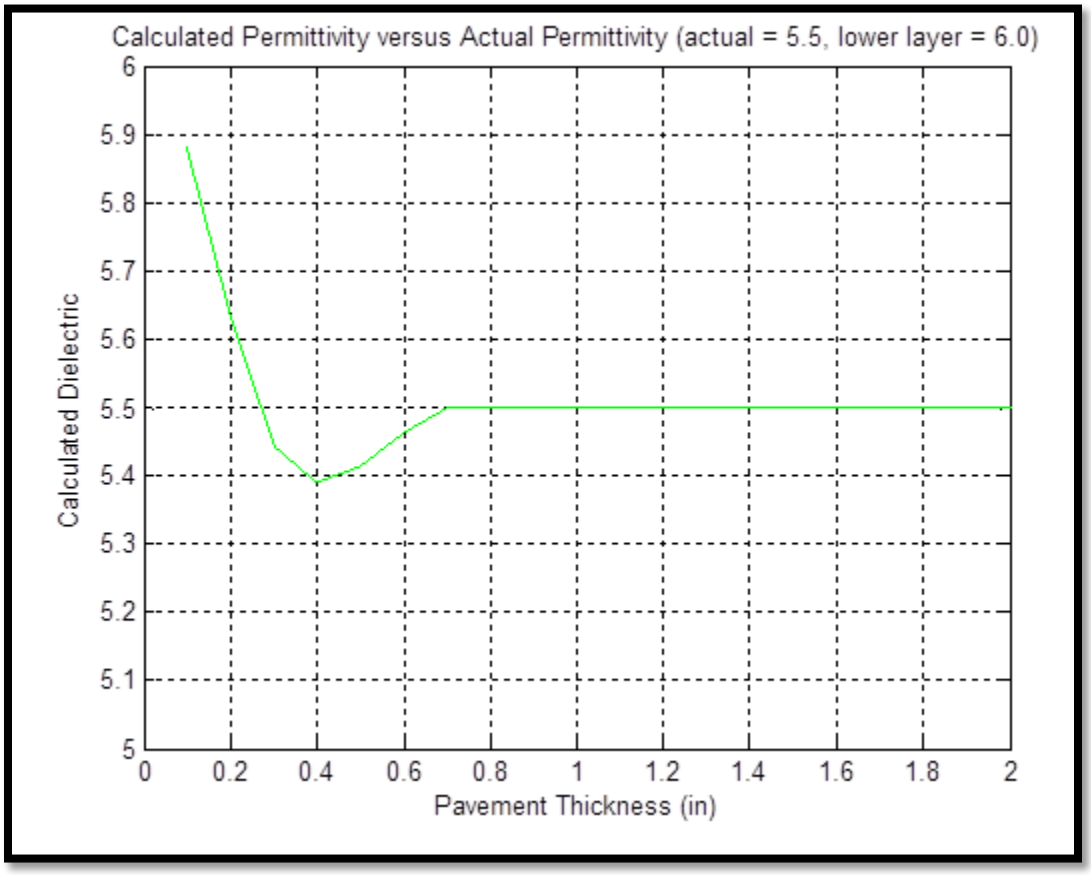

Figure 6. Influence of Surface Layer Thickness on Calculated Surface Layer Dielectric.

Figure 7 illustrates how, in the worst-case scenario, the reproducibility limit would impact calibrations. The reproducibility limit only impacts the intercept of the empirical calibration

equation. Analysis of the curves shows that the 95 percent confidence intervals for the slope coefficients significantly overlap and are not statistically different.

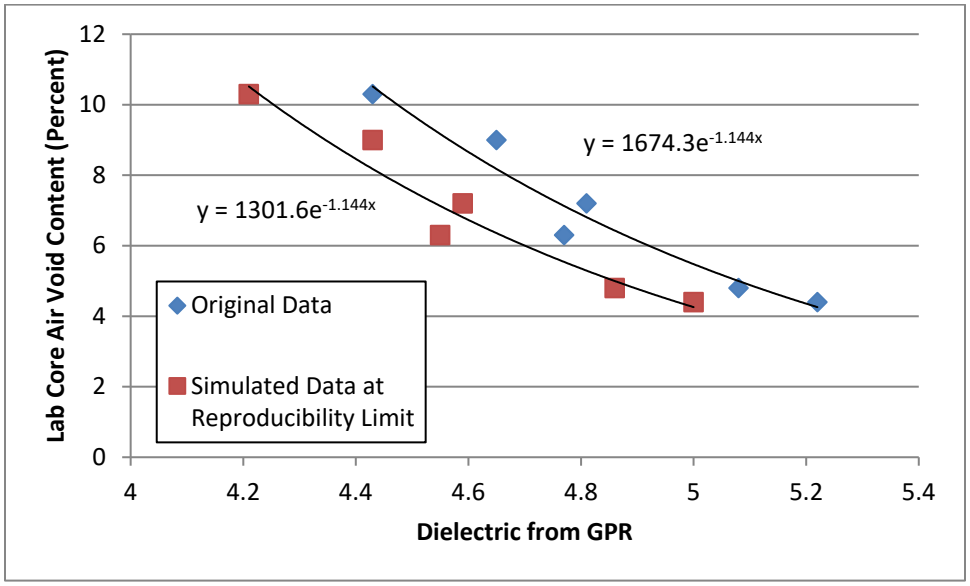

Figure 7. Example Calibration Data from SP 6.33, 1 in. Lift.

Although the simulated calibration curves suggest it may be possible to use one set of calibration factors to air voids for all antennas when the system is used in a multichannel configuration, single factor analysis of variance tests (ANOVA) on the precision data sets show that the different GPR antennas did produce statistically different mean dielectric values for a given asphalt mixture slab. Table 2 illustrates this finding, where the tabulated *F* value exceeds the *F crit* value. These findings suggest that for best results, each antenna may require a unique calibration to density.

Table 2. ANOVA Output for Slab 3, Constant On, Average of 500 Scans.

SUMMARY

Groups	*Count*	*Sum*	*Average*	*Variance*
8	10	60.3506	6.03506	0.00014
7a	10	60.097	6.0097	0.00148
7b	10	59.5374	5.95374	0.00276
3	10	60.0685	6.00685	0.00235

ANOVA

Source of Variation	*SS*	*df*	*MS*	*F*	*P-value*	*F crit*
Between Groups	0.03503	3	0.01168	6.93694	0.00084	2.86627
Within Groups	0.0606	36	0.00168			
Total	0.09563	39				

CONCLUSION

This precision analysis shows:

- In practice, averaging five scans or 500 scans to report the dielectric value does not greatly influence the mean reported surface dielectric constant.
- Increasing the number of scans averaged did improve the precision.
- For materials with dielectrics ranging between 4.4 and 6.4, the dielectric constant measured with the RDM should be repeatable within 0.15 or better and reproducible within 0.22 or better.
- Antenna 7A should be investigated, as the data suggest that antenna may have imprecision and stability problems.

While 500 scans may be feasible for static measurements, in practice, the system would be unable to measure and process this many scans while moving. Therefore, the 5 scan precision statistics are of greater importance, as shown in Table 3 and Table 4.

Table 3. RDM Precision Statistics for Constant on Condition Averaging 5 Scans.

Average Slab Dielectric	Repeatability St. Deviation S_r	Reproducibility St. Deviation S_R	Repeatability Limit r	Reproducibility Limit R
4.37	0.049	0.060	0.14	0.17
5.03	0.051	0.059	0.14	0.17
5.06	0.048	0.078	0.14	0.22
6.01	0.079	0.091	0.22	0.26
6.06	0.069	0.099	0.19	0.28
6.44	0.055	0.14	0.15	0.38

Table 4. RDM Precision Statistics for Hard Reset Condition Averaging 5 Scans.

Average Slab Dielectric	Repeatability St. Deviation S_r	Reproducibility St. Deviation S_R	Repeatability Limit r	Reproducibility Limit R
4.38	0.040	0.041	0.11	0.12
5.02	0.042	0.047	0.12	0.13
5.08	0.044	0.047	0.12	0.13
6.08	0.059	0.093	0.17	0.26
6.11	0.045	0.080	0.13	0.22
6.52	0.049	0.11	0.14	0.31

CHAPTER 4—FIELD DEPLOYMENT AND DATA ANALYSIS

OVERVIEW

The RDM was deployed on six field projects for multiple paving days. In addition to identifying the practicality of routine implementation of the system, researchers evaluated the following topics:

- Reproducibility of calibration curves.
- Precision and bias of the system and nuclear density gage.
- Distribution of predicted void contents.

This chapter first gives the project details and describes the test methods used in the field. Following, the data analysis and results of each topic mentioned above are presented.

PROJECT DETAILS

The RDM was deployed on six construction projects in 2016 and 2017, three in each construction season. Table 5 summarizes details for each project's asphalt mixture design.

Table 5. Project and Asphalt Mixture Details.

Year	Location	Mix Type	Binder Type	Optimum AC (%)	Aggregate Type	Theo. Max SG	Thickness (in.)
2016	US 183 Austin District	TOM-F	PG 76-22	7.2	Sandstone (Delta Mtls)	2.376	0.75
	US 90-Liberty Beaumont District	SP Ty-D	PG 70-22	5.2	Quartzite (Jones Mill) Limestone (Medina)	2.443	1.50
	IH 10-San Antonio S. A. District	SP Ty-C	PG 64-22	5.1	Sandstone (Delta Mtls) Limestone (Servtex)	2.462	2.00
2017	SH 6-Valley Mills Waco District	DG-D	64-22	5.2	Dolomite (Pate) Gravel (Young) RAP	2.447	2.0 (approx.)
	SH 6-Waco Waco District	TOM-C	76-22 + Evotherm	6.6	Sandstone (Brownlee) Dolomite (Marble Falls)	2.434	1.25
	SH 30-College St. Bryan District	SMA-C	76-22	6.0	Sandstone (Brownlee) Dolomite (Servtex) RAP	2.405	2.0

The US 183 project was located in Travis County, and the entire distance of the project was about 2.2 miles (Figure 8). The roadway is a rural, four-lane undivided highway. A TOM-F, with a 9.5 mm nominal maximum size, was placed on top of an existing seal coat, and the lift thickness was 0.75 in. Paving occurred in spring 2016.

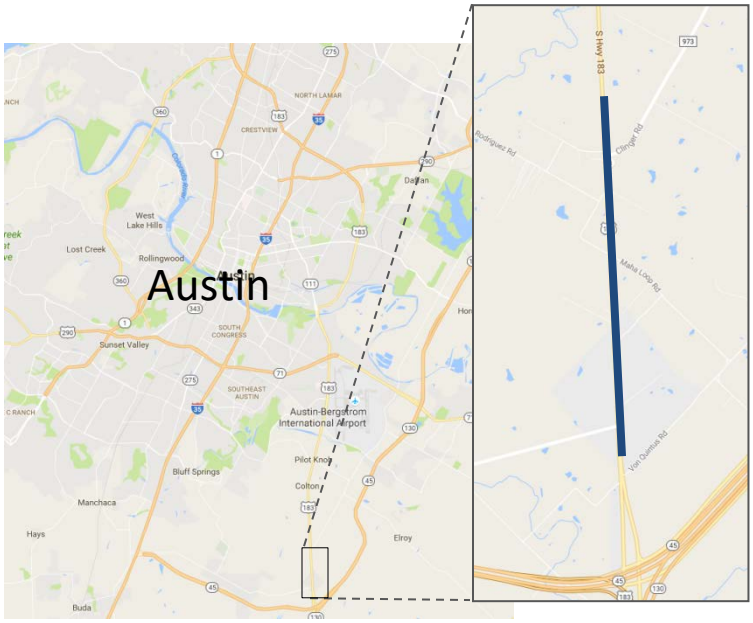

Figure 8. US 183 Project Location.

The US 90 project was located in Liberty, and the entire distance of the project was about 2.6 miles (Figure 9). This roadway is an undivided seven-lane highway, including the center turn lane. A Superpave Type-D mix (9.5 mm nominal maximum size) was laid at a thickness of 1.5 in. after milling the existing HMA. The subsurface pavement was heavily distressed jointed concrete. Paving occurred in late spring 2016.

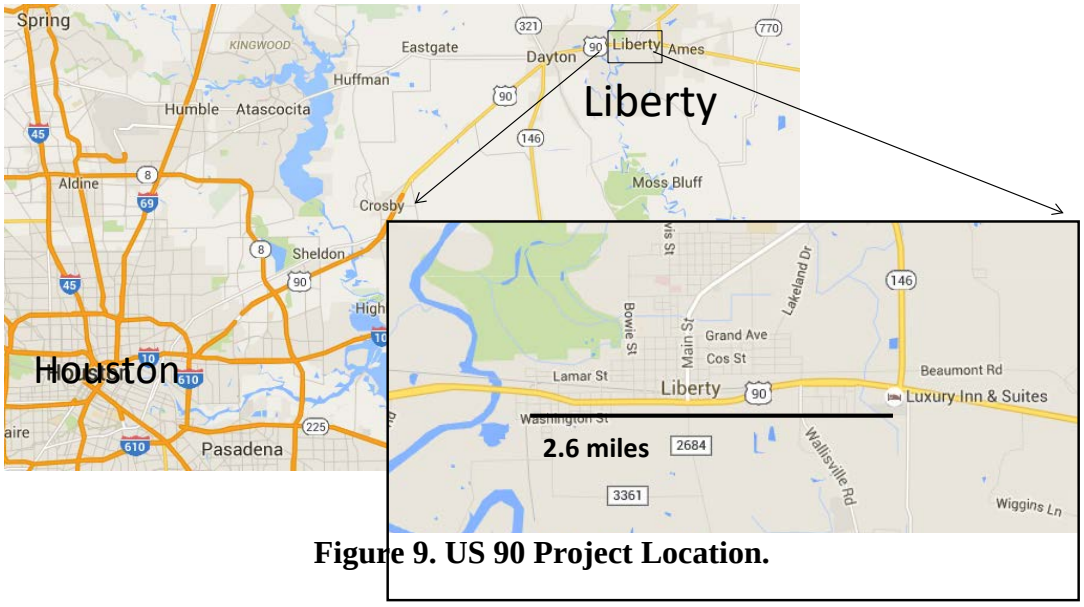

Figure 9. US 90 Project Location.

The IH 10 project was located in east San Antonio starting at Loop 410 and running 2.6 miles in the two left-most west-bound travel lanes (Figure 10). This roadway is a divided six-lane freeway with an annual average daily traffic (AADT) of 72,000. A Superpave C (12.5 mm nominal maximum size) mix with a thickness of 2.0 in. was laid after milling the existing HMA layer. Paving occurred in summer 2016.

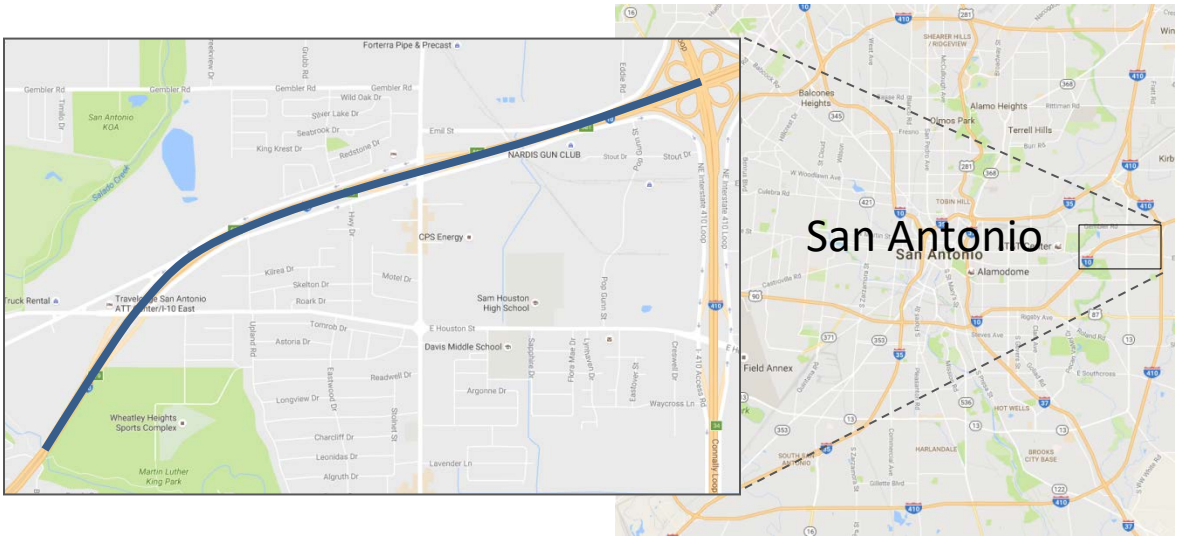

Figure 10. IH 10 Project Location.

The SH 6-Valley Mills project was located outside of Waco, starting at the Valley Mills city limit and running east 10 miles (Figure 10). This roadway is an undivided two-way rural highway with occasional passing and turning lanes. The AADT is about 7,000. A dense-graded Ty-D mix with a thickness of 2.0 in. was laid over existing HMA. Paving occurred in summer 2016. The SH 6-Waco project was located on the south side of Waco, starting at Bagby Ave. and running west 10 miles. This roadway is a divided four-lane freeway with an AADT around 70,000 on the east end and 25,000 on the west end. A TOM-C mix with a thickness of 1.0 in. was laid over a milled surface. Paving occurred in summer 2017.

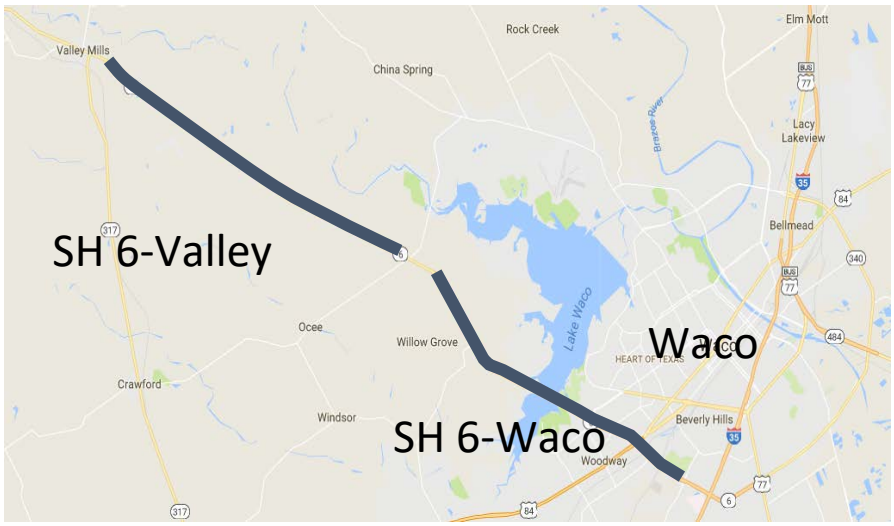

Figure 11. SH 6-Valley Mills and Waco Project Locations.

The SH 30 project was located in College Station between Texas Avenue and SH 6. This roadway is an urban four-lane minor arterial with an AADT of 20,000. An SMA-C mix with a thickness of 2.0 in. was laid over a milled surface. Paving occurred in summer 2017.

Figure 12. SH 30 Project Location.

TEST PROCEDURES

TTI researchers performed density testing on each project for three days or nights of paving (Figure 13). For simplicity, this report calls any given paving period a day. On the first day, they established a 1000-ft test section and measured the surface dielectric with the three-channel RDM over the centerline and both wheel paths. The core-location software identified locations with low, moderate, and high surface dielectric values. At each location, researchers made spot measurements with the RDM by collecting roughly three seconds of data while moving the antenna ±6 in. over the core location. Spot measurements over each location were made with all three antennas, except on US-90, where only one antenna was used for spot measurements. In-place density was then measured using a nuclear density gauge with a 60-second count, followed by coring (Figure 14).

On the second and third days, researchers measured surface dielectric profiles over both wheel paths and the centerline for the majority of paving. The sampling methods varied slightly between the 2016 and 2017 projects. For the 2016 projects, 10 cores were selected at random each time. For the 2017 projects, testing was performed over three sublots, and nine cores were chosen randomly with three in each sublot. For all projects, three of the random cores were specifically taken near the joint. Again, surface dielectric and nuclear density gauge readings were made at each location followed by coring. Loose mixture was sampled on all three days of paving, and TxDOT and contractor QC/QA data were collected. The air void contents of the field cores were measured in the lab. Since lab measured air voids is used for quality acceptance purposes, these values were also considered as true reference values.

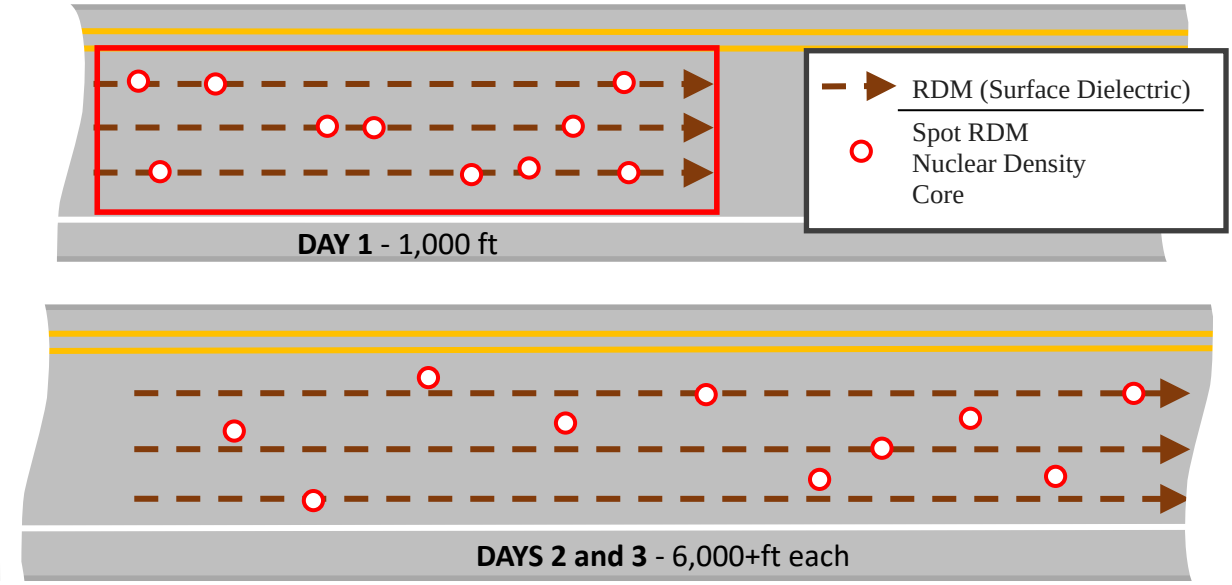

Figure 13. Test Section Layout.
Note: Days 2 and 3 core locations determined from a randomized sampling design.

(a) **(b)** **(c)**

Figure 14. Testing and Sampling: (a) Surface Dielectric, (b) Nuclear Density, and (c) Cores for Bulk Density.

The core and dielectric data were plotted in excel to calculate the calibration coefficients *a* and *b*. The general form of the calibration was an exponential equation, as shown in Equation 2.

$$Voids = ae^{bDiel} \qquad \text{Equation 2}$$

where *Voids* = Core air void content, %.
Diel = Surface dielectric from the RDM.
a, *b* = Calibration coefficients.

Appendix A contains detailed field data.

REPRODUCIBILITY OF CALIBRATION CURVES

The objective of this analysis was to identify which system factors and project factors might affect the calibration curve between surface dielectric and air void contents. Researchers considered the following factors:

- System antenna.
- Paving project (mix design).
- Day of production (fluctuation in produced mix).

The ideal scenario is that the calibration curve will only vary based on the mix design and not on the system antennas or different days of production. Practically speaking, if the calibration curve varies for all factors, then the operator would need unique calibrations for each individual antenna, and the system could require calibration on a daily basis. The second scenario would be particularly cumbersome.

Data Analysis

Two linear models were developed from the variables in Table 6, in the forms of Equations 3 and 4. The core air void data were log-transformed so the data could be analyzed linearly. Table 7 shows the data used for the model. To identify which parameters were statistically significant, an *F* test was performed on each parameter coefficient. If the *p*-value of the predictor variable was lower than the *alpha* level (0.05) than that variable had a statistically significant impact on the core air void content.

Table 6. ANOVA Variables for Reproducibility Analysis.

Response Variable	Variable of Interest	Model Predictor Variables
ln(Core air voids)	Antenna	Dielectric Antenna Project_Day
	Production Day	Dielectric Project Day

$$\ln(Voids) = ß_0 + ß_1 Diel + ß_2 ProjDay_n + ß_3 Ant_n + ß_4 ProjDay_n Diel \quad \text{Equation 3}$$

$$\ln(Voids) = ß_0 + ß_1 Diel + ß_2 Proj_n + ß_3 Day_n + ß_4 Proj_n Diel + ß_5 Day_n Diel \quad \text{Equation 4}$$

where *Voids* = Core air void content, %.
Diel = Surface dielectric from the RDM.

Proj = Project (unique mix design).
Day = Day of production.
ProjDay = Project_Day combination.
Ant = Antenna.
$ß_n$ = Regression coefficients.

One shortcoming of this analysis is that the data collection methods were not identical for each day of paving. Day 1 samples were specifically selected to encompass low, moderate, and high values. On other days, locations were selected randomly. The implication is that if the data happen to be clustered close together, the resulting calibration is less reliable outside the data range.

Table 7. Data Sets Used in Reproducibility Analysis: (a) by Antenna and (b) by Production Day.

(a)

Project	Day	Antenna ID	Sample Size	
			Dielectric	Voids
US 183	1	3, 4, 7	10, 10, 10	10
IH 10	1		10, 10, 10	10
	2		10, 10, 10	10
SH 6-Valley Mills	1		9, 9, 9	9
	2		9, 9, 9	9
	4		6, 6, 6	6
SH 6-Waco	1		9, 9, 9	9
	2		9, 9, 9	9
	3		5, 5, 5	5
SH 30	1		9, 9, 9	9
	2		9, 9, 9	9
	3		9	9
TOTAL			312	104

(b)

Project	Day	Antenna ID	Sample Size	
			Dielectric	Voids
US 183	1	4	10	10
	2		10	10
	3		10	10
IH 10	1		10	10
	2		10	10
	3		10	10
US 90	1		10	10
	2		10	10
	3		10	10
SH 6-Valley Mills	1		9	9
	2		9	9
	4		6	6
SH 6-Waco	1		9	9
	2		9	9
	3		5	5
SH 30	1		9	9
	2		9	9
	3		9	9
TOTAL			174	174

Results

Calibration curves for each project on each day of paving are contained in Appendix A. Figure 15 shows an example of typical calibration curves. The calibrations are good with R^2 values around 0.7. There is some difference among the curve slopes and offsets for different days of paving, though all the data fall within the same general range. Among most of the projects tested, the R^2 values ranged from 0.54 to 0.97, averaging at 0.76. Some production days had much lower correlations, which was primarily caused by limited sampling when paving stopped earlier than expected. Some projects had noticeable shifts in the curves from one day to another, which will be discussed later.

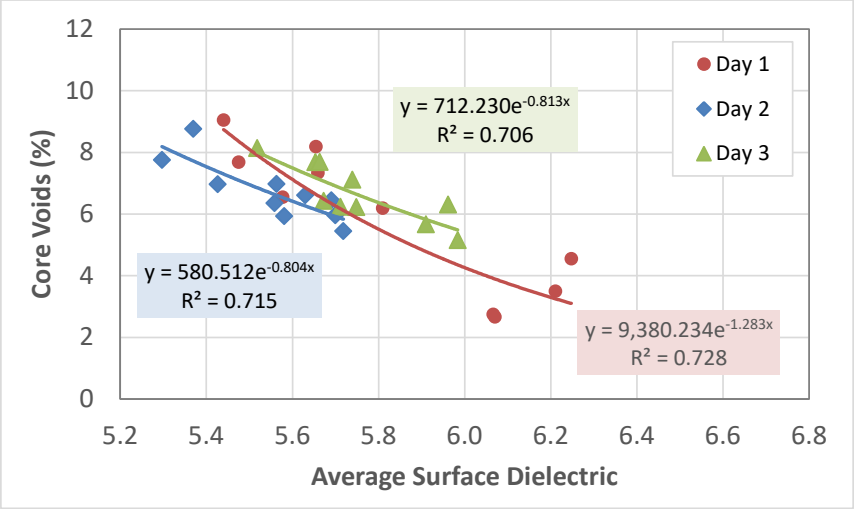

Figure 15. Calibration Curves for IH 10 on Different Days of Paving.

Table 8 gives the statistical result for the effect of the different antennas. Though the calibration curves were heavily influenced by *Dielectric* and *Project_Day* (*p*-values < 0.05), they were not significantly influenced by the *Antenna* factor. This means that the calibration equation generated from one antenna is statistically the same as the calibrations for the other antennas. This is further illustrated in Figure 16, in which the plots for different antennas are hardly visible because they are essentially the same. Therefore, calibrations in the field can be made using a single antenna.

Table 8. Statistical Effect of Different Antennas on Calibration Curves.

Predictor Variable	Model *p*-value	Model R^2	Variable *p*-value	Significant
Dielectric	<0.0001	0.895	<0.0001	Yes
Antenna			0.3111	No
Project_Day			<0.0001	Yes
Project_Day*Dielectric			<0.0001	Yes

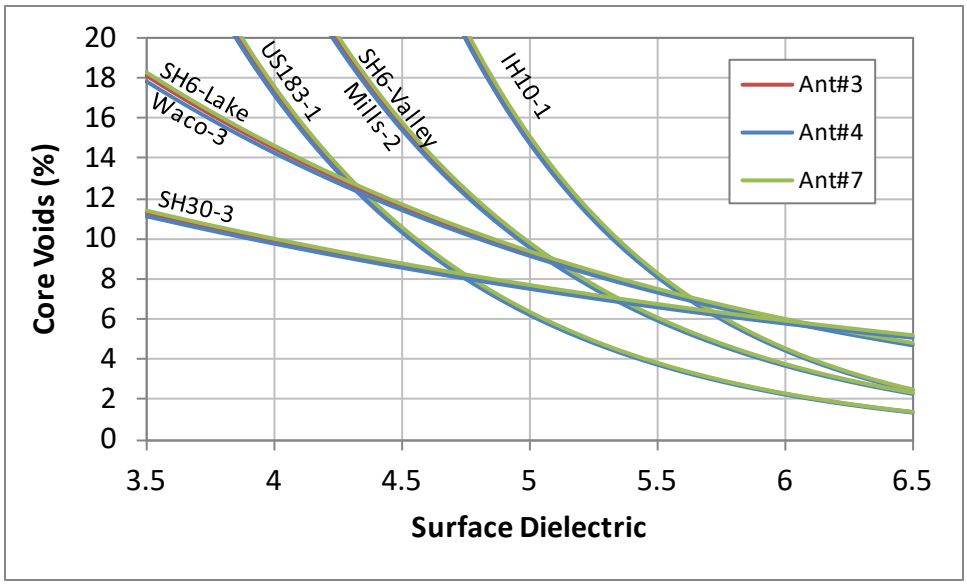

Figure 16. Calibration Curves by *Project_Day* and *Antenna*. (example)

Table 9 and Figure 17 present the change in calibration curves for the production day. This analysis showed that the day of production may have an influence on the calibration curve. The main effect had a *p*-value just above 0.05, and the interaction term was less than 0.05. Some projects did not seem to change from one day to the next, however two projects did have significant changes: SH 6-Lake Waco and SH 30. When the calibration shifts, it could be a result of changes in the produced mix (change in asphalt content, aggregate substitution, etc.). Though researchers sampled plant mix each day and tested the asphalt content and theoretical maximum specific gravity, the variability inherent with each laboratory test makes it difficult to ascribe changes in the calibration to the mixture alone. However, in the case of SH 30 (see Figure 18), the change on Day 3 is so drastic that researchers suspect an error with the system. At present, this is only speculative.

The details of the statistical analyses are found in Appendix B.

Table 9. Statistical Effect of Production Day on Calibration Curves.

Predictor Variable	Model *p*-value	Model R^2	Variable *p*-value	Significant
Dielectric	<0.0001	0.845	<0.0001	Yes
Project			<0.0001	Yes
Day			0.0696	No
Project*Dielectric			<0.0001	Yes
Day*Dielectric			0.0145	Yes

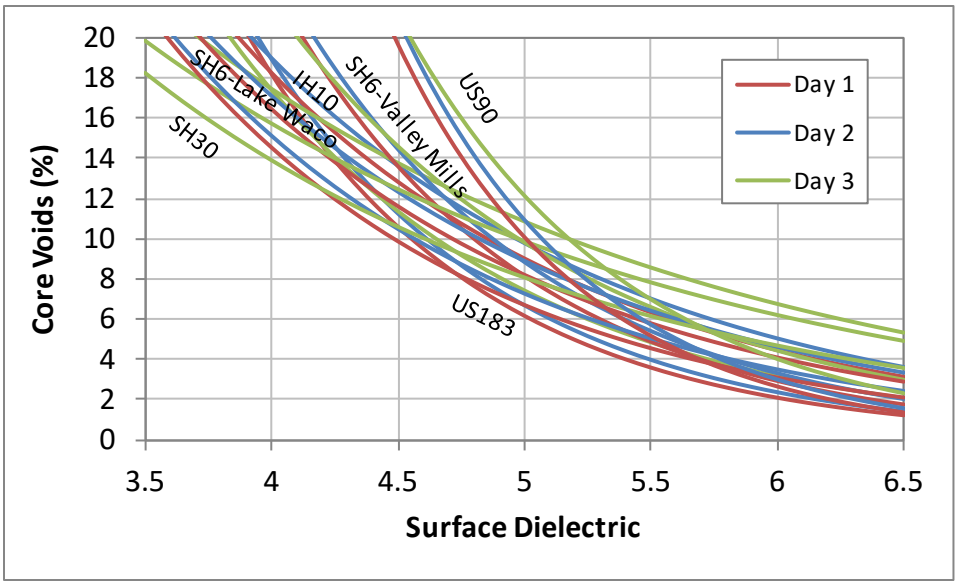

Figure 17. Calibration Curves by *Project* and *Day*.

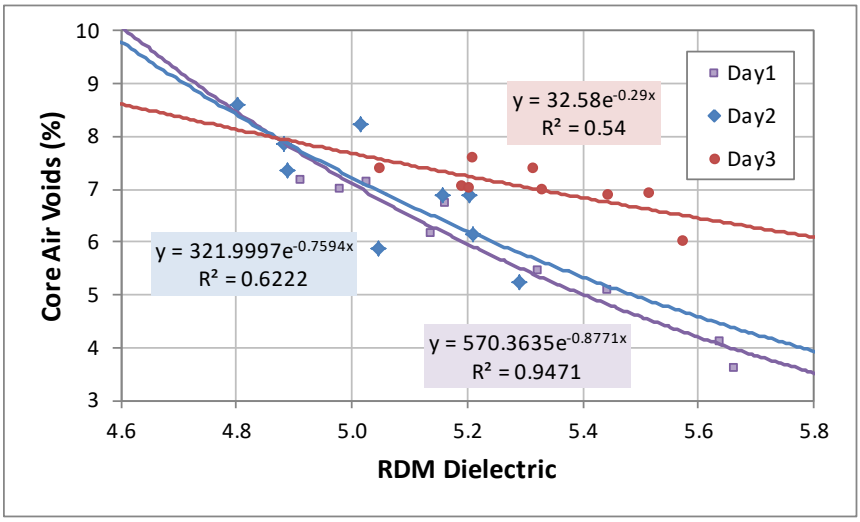

Figure 18. SH 30 Calibrations, Including Potential Outlying Day 3 Calibration.

PRECISION AND BIAS OF RDM AND NUCLEAR DENSITY GAUGE

The objective of this analysis was to quantify the precision and bias of the RDM and current calibration methods. As background, precision describes the consistency of a test method, how clustered together the data are. In the ASTM, precision is defined as the standard deviation of measurements of a given sample. The bias is the difference between the sample average and the true value or reference value.

Data Analysis

The field precision and bias analysis was performed using the data in Table 10. Figure 19 illustrates the analysis methodology. To process the RDM data from each day's production, researchers selected six measurements to establish calibration curves and used the remaining four

measurements for verification. The six calibration measurements were pseudo-randomly selected. Rather than taking six random samples from the 10 cores, researchers randomly picked two samples in the high, moderate, and low dielectric groups, each, as determined by the RDM software and statistical predictions (see Appendix B for details). This random selection process and subsequent data analyses were repeated 1,000 times to ensure a statistically strong representation of all possible calibration and verification scenarios.

Table 10. Data Set Used in Precision and Bias Analysis.

Project	Day	Antenna ID	Sample Size		
			Dielectric	Voids	Nuke
US 183	1	Average of 3, 4, 7	10	10	10
	2		10	10	10
	3		10	10	10
IH 10	1		10	10	10
	2		10	10	10
	3		10	10	10
US 90	1		10	10	10
	2		10	10	10
	3		10	10	10
TOTAL			90	90	90

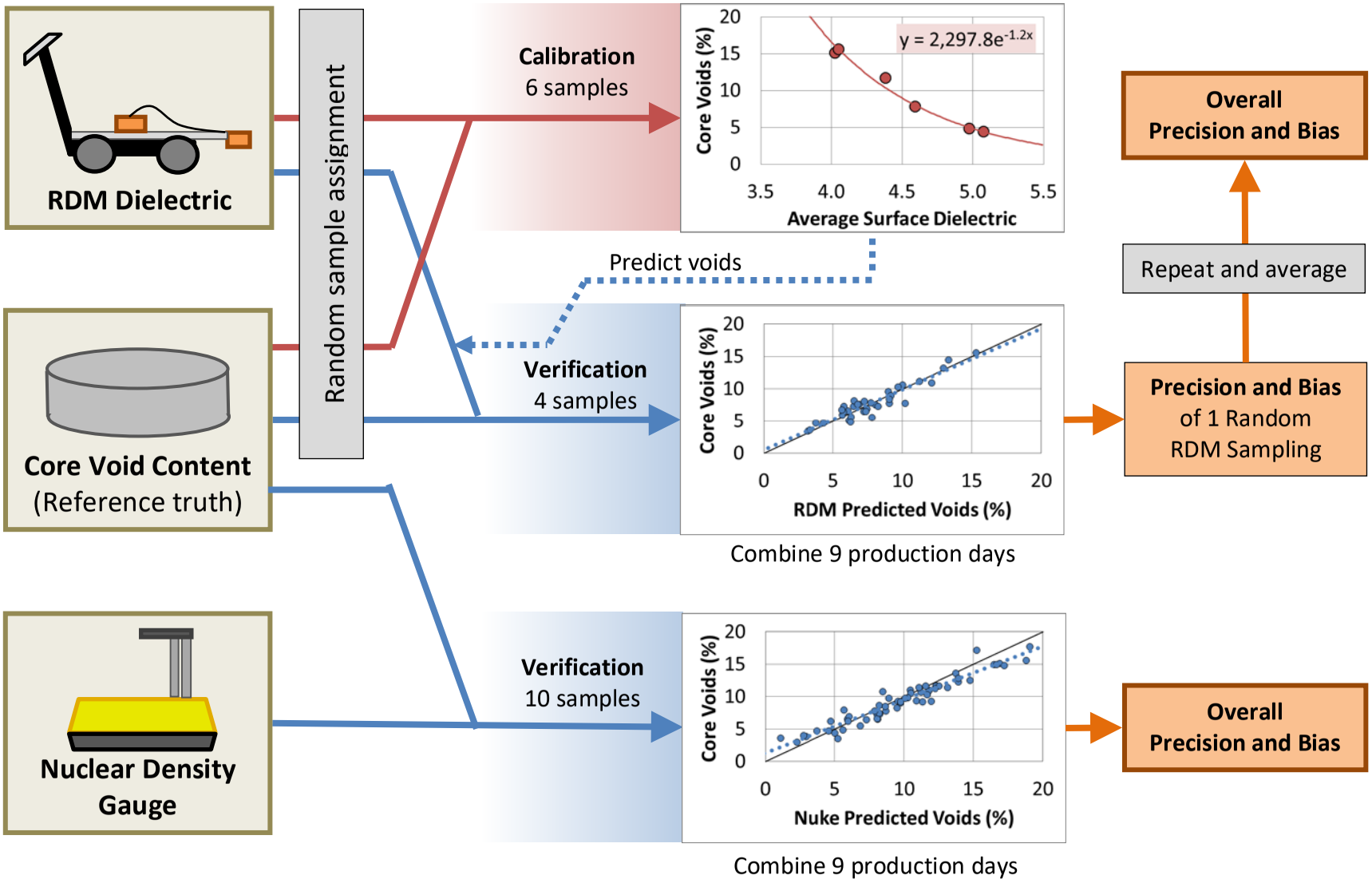

Figure 19. Data Analysis Summary.

Using this calibration, researchers predicted the void content of the remaining four verification locations for each project, and then compared the predictions to the actual core air void contents using a paired t-test. Thirty-six paired samples were evaluated (3 projects × 3 days production × 4 verification measurements). An *alpha* level of 0.05 was used to determine statistical significance, where a *p*-value greater than 0.05 implied the predicted voids and actual voids were not statistically different. Additionally, the data were plotted with a best-fit linear regression line, and the coefficients and R^2 value of the regression equation were evaluated.

The precision and bias were calculated from the residual errors between predicted and actual air void content, in accordance with ASTM E177 (Standard Practice for Use of the Terms Precision and Bias in ASTM Methods). For paired data, precision is the standard deviation of the residual errors, and the overall precision of the RDM was the average of all 1,000 random sample standard deviations (Equation B-1). This calculation and subsequent calculations are detailed in Appendix B. The bias is the difference between the mean test results and the accepted reference value. In our case, the reference values were the core void contents. Bias for each random sample was the average of the residual errors, and the overall RDM bias was calculated as the average of all 1,000 random sample biases (Equation B-2).

The predicted void content of the nuclear density gauge readings was calculated with Equation B-3. In this particular study, the nuclear density gauge was not calibrated to the specific project. Researchers justified this approach since this is not often done in practice. Therefore, all 90 measurements were used to calculate precision and bias (Equations B-5 and B-6, respectively). Had calibration taken place, the slope and bias would be improved, but the scatter would stay the same.

Results

Figure 20 compares the void predictions to the actual void contents. The RDM had a strong correlation with an R^2-value of 0.88. Of equal importance, the regression equation has a slope very close to 1 and a very small offset. This particular graph is just one of the many possible prediction scenarios given different calibration and verification core combinations. For the nuclear density gauge, the correlation had an R^2-value of 0.75 and a noticeable slope and bias.

Table 11 gives the precision and bias results. The bias of the RDM was very near zero, and statistically speaking, a difference was not found between the bias and zero. In comparison, the nuclear density gauge did have a bias of −0.5 percent, and statistically was different than zero. The precision of the RDM was 1 percent, with a confidence interval just under ±2 percent. The nuclear gauge had a precision of 2 percent and confidence of ±3.8 percent.

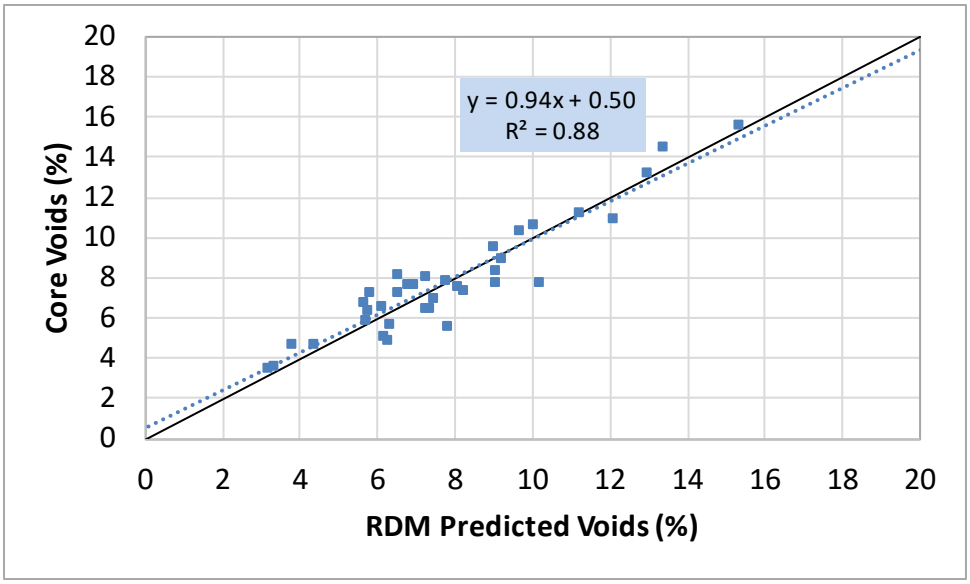

(a)

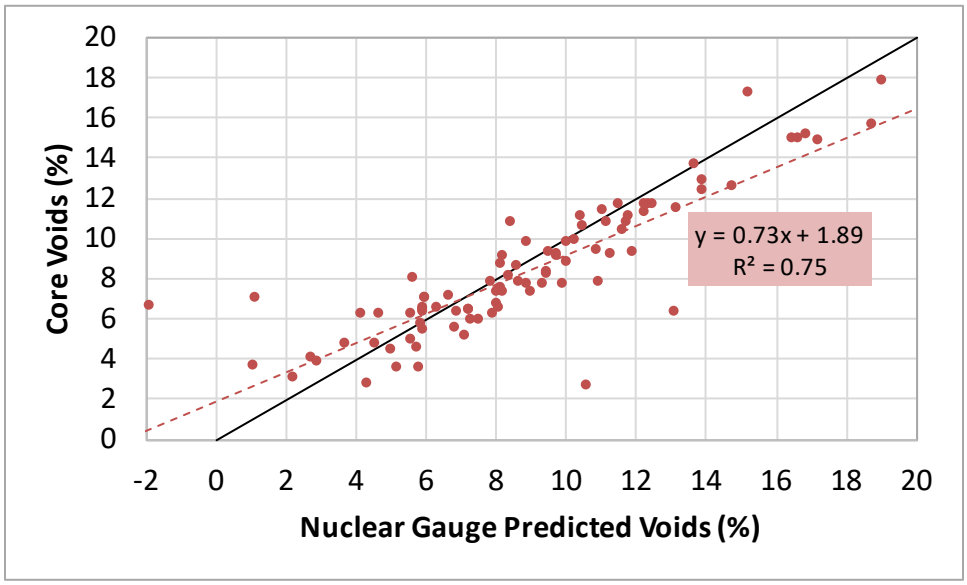

(b)

Figure 20. Void Predictions vs. Actual Core Voids: (a) RDM and (b) Nuclear Gauge.

Table 11. Precision and Bias Results.

Prediction Method	Bias		Precision[2] (% voids)	95% Confidence Interval (% voids)
	Avg. (% voids)	*p*-value		
RDM	0.02	0.463	0.99	0.02±1.94
Nuclear Density Gauge	−0.53	0.012	1.97	−0.53 ±3.84

1 – A value greater than 0.05 is desirable.
(No difference could be found between the prediction bias and zero)
2 – Precision is the standard deviation of the prediction

AIR VOID CONTENT DISTRIBUTIONS

The objective of this analysis was to evaluate the predicted air void content distributions of each project. Consideration was given to air void predictions using first day calibrations vs. daily calibrations. Also, the different air void distributions within specific longitudinal profiles were evaluated: left wheel path, between wheel paths, right wheel path, and joints.

Data Analysis

Table 12 shows the data set used for the void distribution analyses. The projects tested in 2016 are subdivided by day while the 2017 projects are subdivided by lot and sublot. All sections have data for both wheel paths and between wheel paths. Select locations also have joint data.

Table 12. Data Set for Void Distribution Analysis.

Project	Day	Lot	Sublot	Profile Location		Measured Distance (ft)
				WPs and BWP	Joint	
US 183	1	NA	NA	Yes	Yes	1,000
	2				Yes	6,800
	3					6,100
IH 10	1				Yes	1,000
	2					6,000
	3					6,200
US 90	1				Yes	1,000
	2					6,800
	3					6,200
SH 6-Valley Mills	1	6	1		Yes	4,700
	2	8	1,2		Yes	10,800
	3	9	1			3,100
	4	11	1,2			5,800
SH 6-Waco	1	2	1		Yes	3,800
	2	3	1, 2, 3			11,000
	3	8	1,2			5,000
SH 30	1	1	1		Yes	1,000
	2	3	1,2,3		Yes	5,700
	3	4	2,3,4			5,700
					Total	19.2 mi

For each period of paving equal to or larger than a sublot, histograms of air void content and summary statistics were calculated. The summaries included the average, standard deviation, 5^{th}, 50^{th} (median), and 95^{th} percentile void content. Lastly, the density profiles within the wheel paths, between the wheel path, and along the joint were compared with paired t-tests.

Results

Predicted Void Distribution

The air void distribution graphs for each project are illustrated in Figure 21 and Figure 22, and the summary statistics given in Table 12. The air void contents varied significantly among the projects and within each project for different paving periods. In most cases, this reflects actual changes in air voids within the project. In some cases, however, it may be more related to errors in establishing the calibration curve, like SH 30 Lot 4. The highest void contents were for the two TOM projects, US 183 and SH 6-Lake Waco, with average void contents around 12 and 10 percent, respectively. The best uniformity was on the SH 30 project, with an overall standard deviation around 0.5 percent.

Table 13. Summary Statistics for Each Project.

Project	Day	Lot	Sublot	Air Voids %				
				Average	St. Dev.	Percentile		
						5th	50th (median)	95th
US 183	2	NA	NA	11.4	1.85	8.6	11.5	14.2
	3			12.1	1.85	9.4	12.0	15.3
IH 10	2	NA	NA	6.2	0.78	4.9	6.2	7.5
	3			7.3	0.77	6.1	7.2	8.5
US 90	2	NA	NA	7.3	1.47	5.1	7.2	9.8
	3			8.2	1.37	6.2	8.1	10.6
SH 6-Valley Mills	1	6	1	6.8	1.00	5.4	6.7	8.6
	2	8	1	8.4	1.38	6.4	8.3	10.7
			2	8.5	1.17	6.8	8.4	10.4
	3	9	1	7.5	1.45	5.8	7.2	10.3
	4	11	1	6.8	0.80	5.6	6.8	8.0
			2	6.7	0.62	5.7	6.7	7.7
SH 6-Lake Waco	1	2	1	11.9	1.27	10.2	11.8	14.1
	2	3	1	9.1	1.32	7.0	9.1	11.2
			2	10.1	1.21	8.3	10.0	12.1
			3	9.9	1.40	7.6	9.9	12.1
	3	8	1	10.9	1.09	9.4	10.8	13.0
			2	11.0	0.86	9.8	11.0	12.5
SH 30	2	3	1	5.9	0.75	4.7	5.8	7.2
			2	6.4	0.52	5.6	6.4	7.3
			3	6.4	0.51	5.6	6.4	7.2
	3	4	2	7.1	0.31	6.5	7.1	7.5
			3	7.0	0.35	6.5	7.0	7.5
			4	6.9	0.31	6.4	6.9	7.4

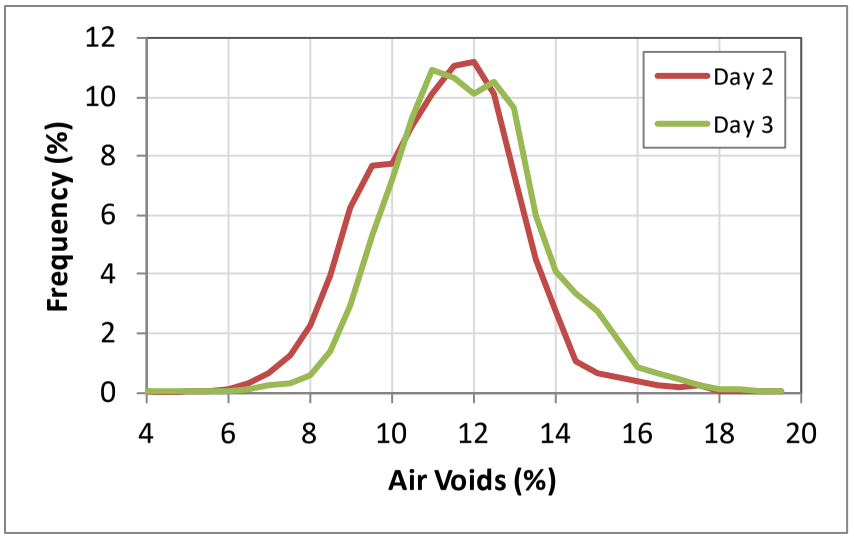

(a)

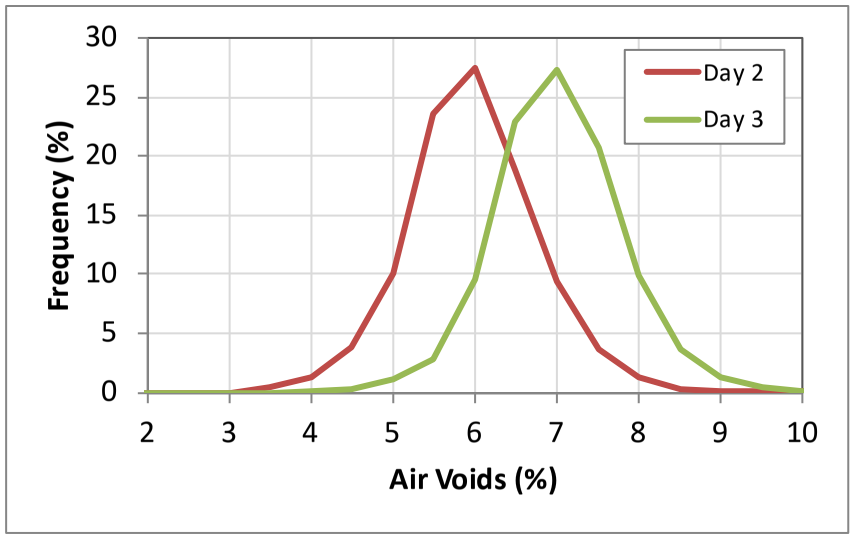

(b)

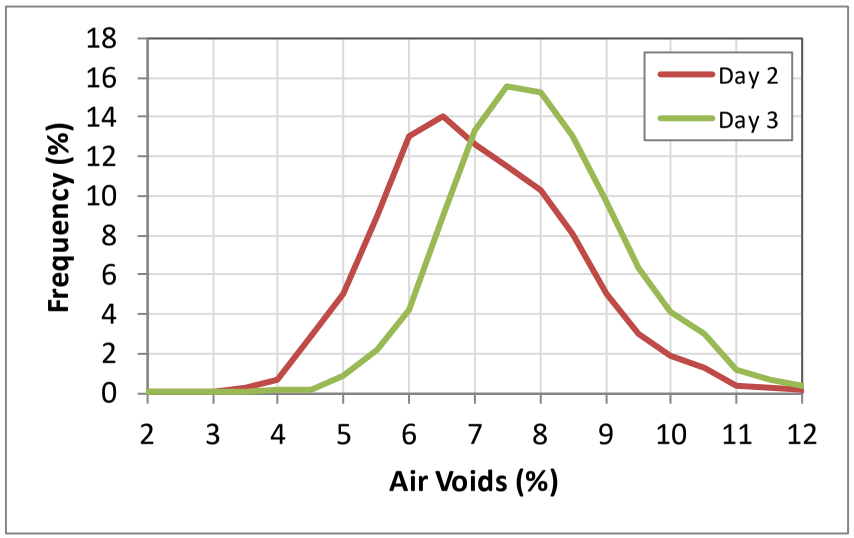

(c)

Figure 21. Distribution of Air Voids by Day: (a) US 183, (b) IH 10, (c) US 90.

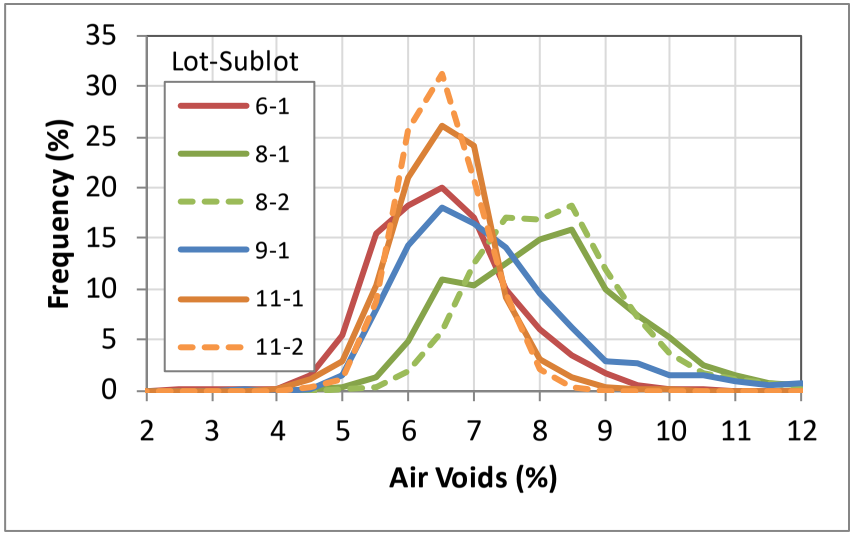

(a)

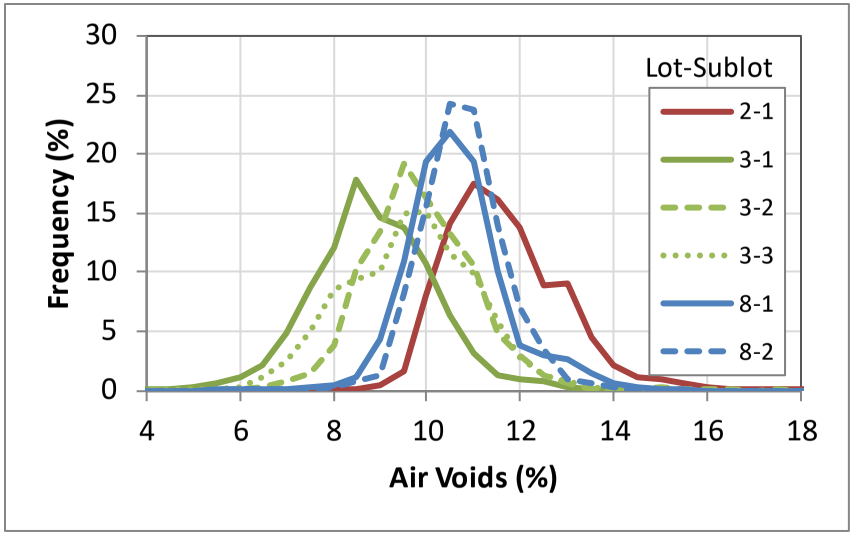

(b)

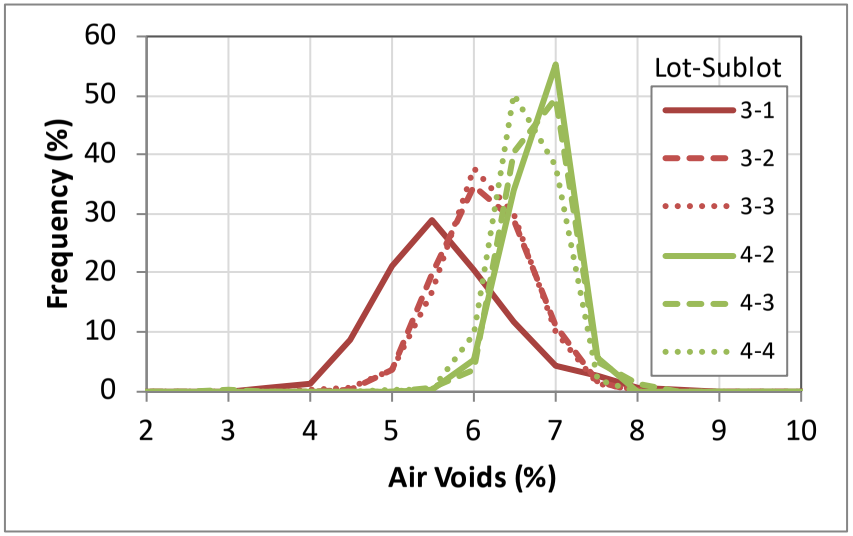

(c)

Figure 22. Distribution of Air Voids by Lot and Sublot: (a) SH 6-Valley Mills, (b) SH 6-Lake Waco, (c) SH 30.

Line-Scan Variability

Based on paired t-tests among predicted void contents in and between the wheel paths, the line scans are not the same (p-value < 0.001). Figure 23 shows an example set of scans. While there may be a very general trend in the data, one line scan may be lower or higher than others at various times. What this means is that testing one line scan of the pavement is insufficient to characterize the overall pavement density. This is largely because of roller patterns. Often the highest density is in the center of the mat because of roller overlap. Also, a roller will often compact one side of the mat first while the other side cools down significantly, making it more difficult to compact the second side.

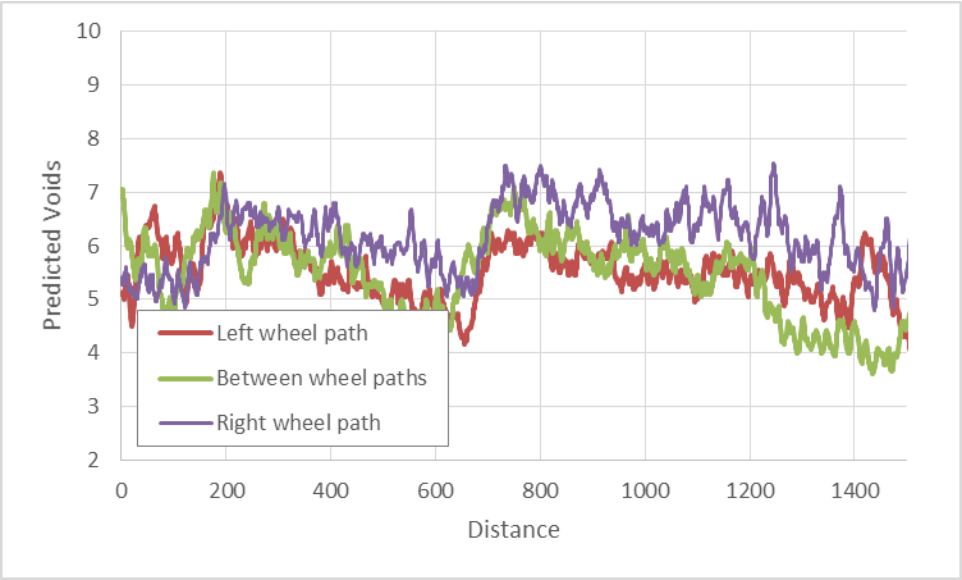

Figure 23. Example Comparison of Line Scans (SH 30-College Station-TOM).

CONCLUSION

Reproducibility of Calibration Curves

Overall air void calibrations were good with an average R^2 value of 0.76. The calibration curves were unique for different paving projects (i.e., different mix designs). In some cases, the curves also changed on different days of paving, which suggests there was variability in the mix produced (e.g., change in asphalt content). In one case, there may have been an equipment error with the RDM. Even though there are differences among antenna readings, the difference was not large enough to affect the overall calibration curves.

Field Precision and Bias

The RDM had negligible bias and a precision of 1 percent voids. For a given reading, the true value is expected to lie within ±2 percent voids (with 95 percent confidence). The nuclear density gauge had a bias of −0.5 percent and precision of 2 percent. The expected true value as

measured from the gauge would be within −0.5±3.8 percent voids. The RDM is more precise than the nuclear density gauge and unbiased.

Air Void Content Distributions

The air void contents varied significantly among different projects, and most projects had significant variation from day to day. Some of this variation is directly related to changes in the mat density, while errors in establishing the calibration curves would also create a significant shift in the predicted voids. The air voids also varied within different line profiles. The lowest voids were measured between the wheel paths where rollers overlap, and the highest voids were measured at the longitudinal joints.

Recommendations

Recommendations are as follows:

- Establish a new calibration curve for each project with a unique mix design.
- For multichannel RDM systems, designate a single antenna for establishing the calibration curves.
- During routine testing, use the following thresholds to trigger establishing a new calibration curve (these are subject to change as they do not have a research basis):
    - A discrepancy greater than 2 percent air voids between the RDM and core measurements.
    - Change in the job mix formula.
- During research testing, recalibrate the system for each day of paving.
- For general density profiling, test both wheel paths and between the wheel path. Strong consideration should be made to also test the longitudinal joint.

Recommended future research:

- Perform a sensitivity analysis of mix design parameters in a laboratory environment to determine the correct thresholds to warrant a new calibration curve.
- Investigate mechanistic and mechanistic-empirical models relating the dielectric to air void content that also account for changes in the mix design.

CHAPTER 5—ESTIMATION OF PRODUCER AND CONSUMER RISK

OVERVIEW

The acceptance and payment of asphalt mixture construction has inherent risk to the agency and the contractor. The agency (consumer) is at risk of accepting production when in fact the pavement has significant poorly constructed areas. This is a statistical Type II error. On the other hand, risk to the contractor (producer) occurs if the production is penalized when the large majority of the construction actually had acceptable quality (a statistical Type I error).

The predicted void content data and random core QA data were used to estimate user and producer risk with and without the extensive testing coverage of the RDM system. This chapter first gives the analysis methods, presents the analysis results, and concludes with recommendations.

METHODS

The data from the following four projects in Table 14 were used in the risk analysis. Data from the two TOM mixes were not considered because the current specification accepts construction based on the flow time test and not the void contents of cores.

Table 14. Data Set for Risk Analysis

Project	Day	Lot	Sublot	Sample Size	
				Cores	RDM System (ft)
IH 10	2	NA	NA	3	6,000
	3			3	6,200
US 90	2			3	6,800
	3			3	6,200
SH 6-Valley Mills	1	6	1	1	4,700
	2	8	1,2	1	10,800
	3	9	1	1	3,100
	4	11	1,2	1	5,800
SH 30	2	3	1,2,3	1	5,700
	3	4	1,2,3	1	5,700

Possible payment outcomes were predicted for each paving period. The outcomes were calculated based on the void predictions and the payment adjustment factors for in-place air voids for dense-graded HMA (Item 341), Superpave HMA (Item 344), and SMA (Item 346). Outcomes included:

- Weighted average (payment based on everything placed).
- 50th percentile (payment for the average).
- Average of the 5th and 95th percentile (payment based on average of worst and best areas).

In the calculations, measurements in the remove and replace range were assigned a pay factor of 0.0. The resulting pay factors were compared to the actual project pay factors as determined by coring. These data came from contractor core results and also from random coring by TTI.

Producer and consumer risk were evaluated based on the air void sample size (number of measurements) for a given tolerable testing error and project variability. Equation 5 shows the relationship of these parameters (*18*).

$$n = \frac{(Z_{\alpha/2} + Z_{\beta})^2 \sigma^2}{e^2}$$ Equation 5

where n = Number of air void content samples.
$Z_{\alpha/2}$ = Z-critical value for producer risk.
$Z_{ß}$ = Z-critical value for consumer risk.
α and ß = Producer and consumer risk, respectively.
Between 0.0 (willing to accept no risk) and 1.0 (willing to accept all risk).
s = Standard deviation of void content within a project.
e = Tolerable error in the average result.

The standard deviation chosen for this analysis was 1.4 percent air voids. This value corresponds to the 80th percentile standard deviation of air voids among all the projects and paving periods in this study (Figure 24). Meaning, 80 percent of projects and paving periods tested had an air void standard deviation of 1.4 percent or less.

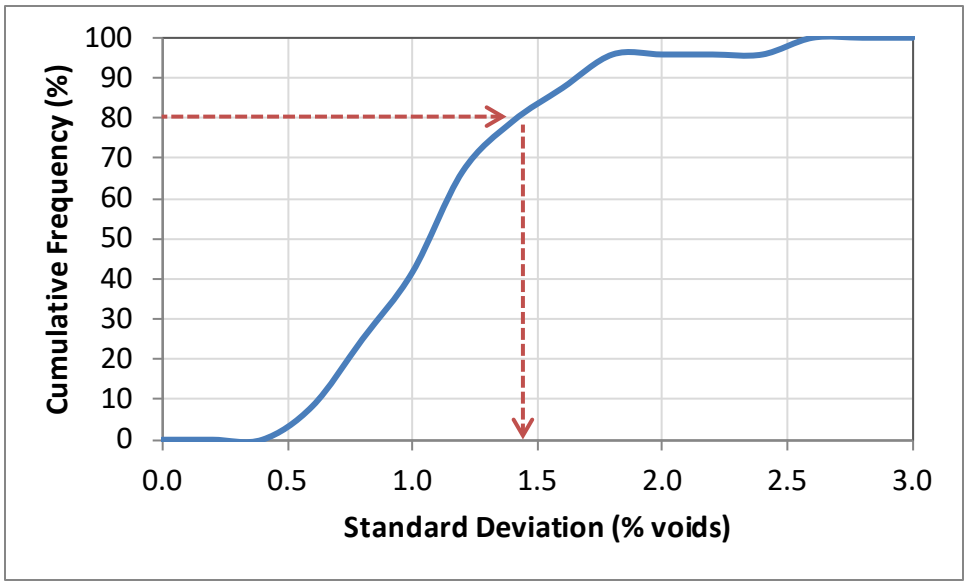

Figure 24. Cumulative Frequency of Standard Deviations for Project Void Contents.

A range of tolerable errors were used in the analysis. Considering that pay factors change every 0.1 percent voids, and that the range of full bonus is only 1 percent voids, a small tolerance of 0.1 percent was used on the low end. A tolerance of 3 percent voids was used on the high end, which lacks the ability to distinguish among pay factor criteria.

RESULTS

Table 15 gives the pay factors based on simple core samples and the RDM. Statistically speaking, the pay factor from the random core should be closest to the 50th percentile pay factor. The weighted average pay factor, which considers the void results of the full mat, was considerably lower for certain paving periods, and equal to or slightly higher for other periods. The 5th and 95th average pay factor was much lower than the other factors because the payment is calculated from on the lowest performing areas. These pay factors are heavily dependent on achieving a good calibration before testing. Any errors in the calibration will result in errors in the readings and in the final pay factor.

Table 15. Possible Payment Outcomes.

Project	Day	Lot	Sublot	Pay Factor			
				Core (current method)	Weighted Avg.[1]	50th Percentile	5th and 95th Avg.[1]
IH 10	2	NA	NA	1.00[2]	1.04	1.04	1.04
	3			1.07[2]	0.97	1.01	0.92
US 90	2	NA	NA	1.02[2]	0.87	1.01	0.54
	3			Reject[2]	0.70	0.88	0.52
SH 6-Valley Mills	1	6	1	1.02	1.03	1.04	1.03
	2	8	1	1.03	0.87	1.00	0.52
			2	1.03	0.90	1.00	0.52
	3	9	1	1.05	0.96	1.03	0.53
	4	11	1	1.05	1.03	1.04	1.03
			2	1.05	1.04	1.04	1.03
SH 30	2	3	1	1.02	1.04	1.06	1.02
			2	0.76[2]	1.03	1.04	1.01
			3	1.10	1.03	1.04	1.01
	3	4	2	1.04	0.97	1.00	0.94
			3	1.07	0.97	1.00	0.94
			4	1.01[2]	0.99	1.01	0.97

1 - Reject areas assigned a pay factor of 0.0.
2 – TTI cores. Other values based on contractor QA cores.

Another approach to characterizing compaction quality is percent within limits (Table 16). All the projects tended to have air voids above the target full bonus range. The highest voids were estimated on US 90 (11 to 23 percent in reject) and SH 6-Valley Mills (11 percent reject.) The best compacted project was SH 6-Valley Mills-Lot 6 with 24 percent full bonus. Overall, the projects had less than 2 percent below the target (over compaction), 8 percent at the target, 68 percent with an above target bonus, and over 20 percent in the above target penalty and reject category.

Table 16. Percent within Limits Outcomes.

Project	Day	Lot	Sublot	Percent Within Limits						
				Below Target			Target	Above Target		
				Reject	Penalty	Bonus	Full Bonus	Bonus	Penalty	Reject
IH 10	2	NA	NA	0.0	0.1	0.7	6.1	88.6	4.3	0.1
	3			0.0	0.0	0.0	0.4	68.2	29.9	1.6
US 90	2	NA	NA	0.2	0.2	0.4	4.1	55.4	28.9	10.9
	3			0.2	0.1	0.1	0.3	32.5	43.3	23.6
SH 6-Valley Mills	1	6	1	0.0	0.3	1.8	24.0	69.0	4.8	0.1
	2	8	1	0.0	0.0	0.0	2.0	56.9	29.5	11.5
			2	0.0	0.0	0.0	0.5	57.7	33.7	8.1
	3	9	1	0.0	0.1	0.2	12.5	71.0	10.2	6.1
	4	11	1	0.0	0.0	1.4	17.0	80.0	1.4	0.2
			2	0.0	0.0	0.3	13.8	85.8	0.1	0.0
SH 30	2	3	1	0.0	0.1	0.2	12.7	80.4	6.1	0.5
			2	0.0	0.0	0.0	0.4	90.4	9.2	0.0
			3	0.0	0.0	0.0	1.0	91.0	7.9	0.1
	3	4	2	0.0	0.0	0.0	0.0	51.7	48.3	0.0
			3	0.0	0.1	0.0	0.1	57.8	41.3	0.8
			4	0.0	0.0	0.0	0.0	71.9	28.1	0.0
Average				0.0	0.4	1.1	8.1	68.1	18.9	3.3

Figure 25 and Figure 26 show the risk analysis results for producers and consumers, respectively. Though hard to distinguish in the graphs, the overall risks are higher for the producer. For a given error tolerance, increasing the number of samples reduces the risk. Also, increasing the samples at a given level of risk increases the overall confidence of the measurement.

To help interpret the graphs, consider the following example. Under the present conditions, only one sample is tested per sublot. To accept paving based on a single core location, and assuming the overall average air void content is within 2 percent of the reading, TxDOT must also accept a 40 percent chance of incorrectly accepting the project. On the other hand, since the RDM produces such a rich set of data, often over 10,000 readings per sublot with a 3-channel system, TxDOT can lower their risk to well below 10 percent, and have confidence that the measured average air voids are within 0.1 percent of the true mean.

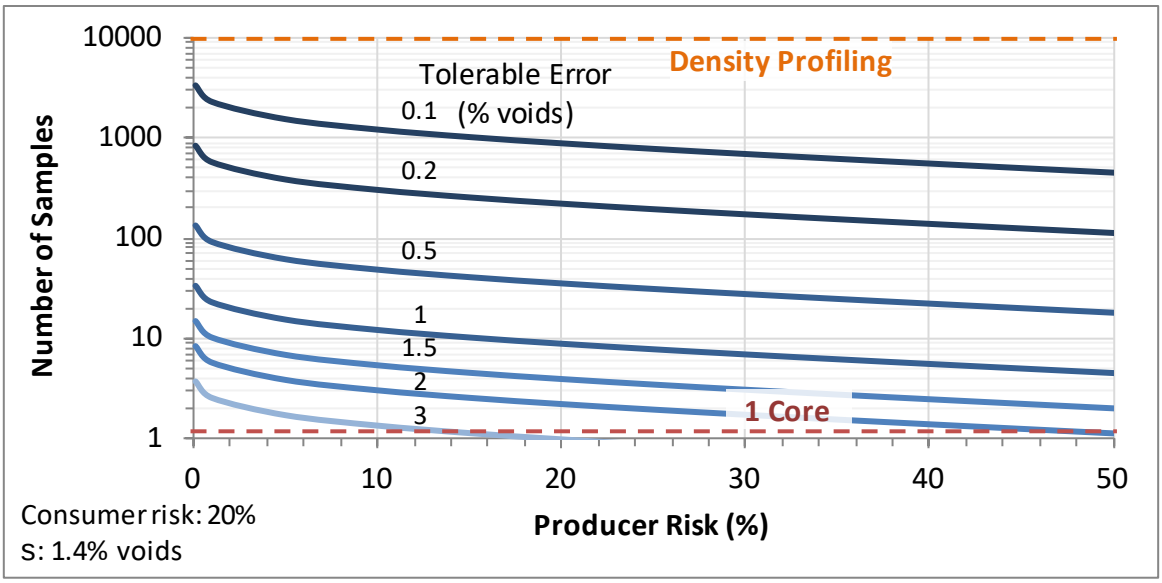

Figure 25. Number of Samples vs. Producer Risk and Tolerable Error.

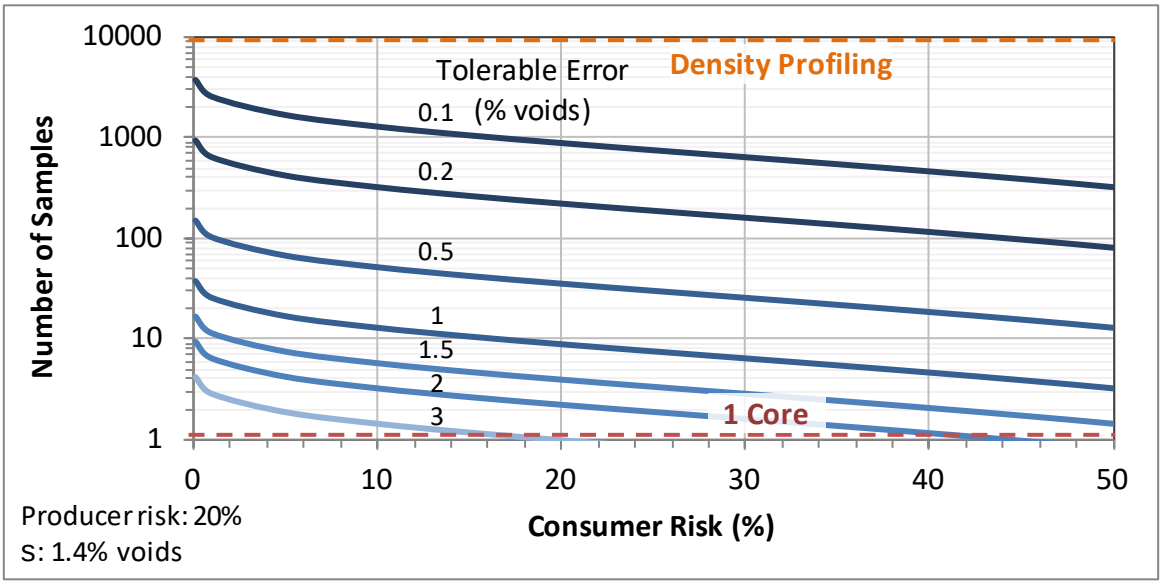

Figure 26. Number of Samples vs. Consumer Risk and Tolerable Error.

CONCLUSION

On certain projects and paving periods, the weighted average pay factor was considerably lower than the pay factor from random coring. But on other projects the weighted pay factor was equal to or slightly higher. The pay factor from the average of the 5th and 95th percentile heavily weights the worst areas and results in a pay factor much lower than the other approaches.

These pay factors are heavily dependent on achieving a good calibration before testing. Any errors in the calibration will result in errors in the readings and errors in the final pay factor. Based on a percent within limits characterization, overall the projects had less than 2 percent below the target (over compaction), 8 percent at the target, 68 percent with an above target bonus, and over 20 percent in the above target penalty and reject category.

Based on the producer and consumer risk analysis, the overall risks are higher for the producer. For a given error tolerance, increasing the number of samples reduces the risk. Also, increasing the samples at a given level of risk increases the overall confidence of the measurement. The RDM could provide a viable approach to significantly increasing testing coverage, thus reducing producer and consumer risks and reducing acceptance error.

CHAPTER 6—DEPLOYMENT OF 3D RADAR

OVERVIEW

While the majority of the work performed in this project focused on a 3-channel GPR system tailored for measurement of asphalt mixture density (Figure 27b), this project also performed a limited evaluation of a 32-channel radar system (Figure 27a). Researchers used a vehicle-mounted air-coupled GPR system, comprised of 32 channels of step-frequency antennas. This system continuously measures pavement layer properties stepping at 10 MHz intervals from 150 to 3,000 MHz. The system used has an effective measurement width of approximately 5 ft 2 in. This data collection arrangement results in a high-resolution 3D scan of the pavement structure.

Researchers deployed the 3D radar system on three test sections: one existing section maintained by TTI, and on SH 6 and SH 30 construction projects. The goal of this deployment was to determine if it may be feasible to predict HMA density in a quality control or assurance scenario with the 3D radar.

(a) **(b)**

Figure 27. Radar Systems: (a) 3D Radar and (b) RDM.

METHODOLOGY

The 3D radar system was deployed on a test section on Texas A&M's RELLIS (formerly Riverside) campus. The system was also deployed shortly after construction of overlays on SH 6 near Valley Mills and on SH 30 in College Station. Table 17 gives details for these projects.

Table 17. Project and Asphalt Mixture Details.

Project ID	Mix Type	Binder Type	Optimum AC (%)	Aggregate Type	Theo. Max SG	Thickness (in.)
RELLIS	DG-C	76-22	4.8	Limestone (Hanson)	NA	2.0
SH 6-Valley Mills	DG-D	64-22	5.2	Dolomite (Pate) Gravel (Young) RAP	2.447	2.0
SH 30-College Station	SMA-C	76-22	6.0	Sandstone (Brownlee) Dolomite (Servtex) RAP	2.405	2.0

Researchers collected 3D radar data over the entire RELLIS test section, over sublots on SH 6, and over a 1,000 ft calibration section on SH 30. As feasible under live traffic conditions, data were also collected over a longitudinal construction joint. Table 18 summarizes the data collection parameters.

Table 18. Data Collection Parameters

Radar Data	
Domain	Frequency
Min. Frequency	150 MHz
Max Frequency	2990 MHz
Freq. Step	10 MHz
Time Window	50 ns
Dwell Time	0.55 µs
Trigger	
Mode	Distance
Sampling Interval	12-in. (SH 6)
	3-in. (SH 30)

A preliminary analysis of the data was performed using the equipment manufacturer's software, as summarized in Table 19.

Table 19. Post-Processing Steps.

Process	Parameters
Add 3D Radar Files	All files collected
Process Selected Regions	Initial processing of all files
Region Process Settings – Time Ground (ns)	3.929
Set the dielectric (Epsilon)	5
Turn on Filters: Interference Suppression Automatic Ground Alignment ISDFT Autoscale BGR (Background removal) (high pass) BGR (mean)	 10 dB 3.929 ns Attenuation 0.01; Kaiser beta 6 Default settings Filter length 100; BGR removal 100%; start depth 3.929 ns BGR removal 100%

A critical part in determining HMA density from radar signals is using the surface reflection signal and the metal plate reference signal to estimate the material dielectric (Equation 1).

In its current form, the software is unable to analyze the frequency domain radar signal in this fashion; therefore, a direct calculation of the dielectric and thus density prediction was not possible.

RESULTS

Figure 28 and Figure 29 give example results from SH 6 and SH 30. The first image shows the uniformity of the overlay surface over one sublot. The sublot was uniform at the beginning and end, with some areas have more or less compaction than others. Some of the anomalies may be patched core holes. In Figure 28, the color values are not actual density values, but just a representation of changes in the antenna signal. To obtain actual density values, custom data processing steps not yet developed must be introduced into the software.

The two plots in Figure 29 from SH 30 illustrate an advantage of the 3D radar compared with the RDM. Since the 3D system measures layer properties with depth, the user can examine the overlay both at the surface and at the bottom of the lift. The non-uniformity near 2.5 in. deep may be attributed to uneven milling or uneven compaction.

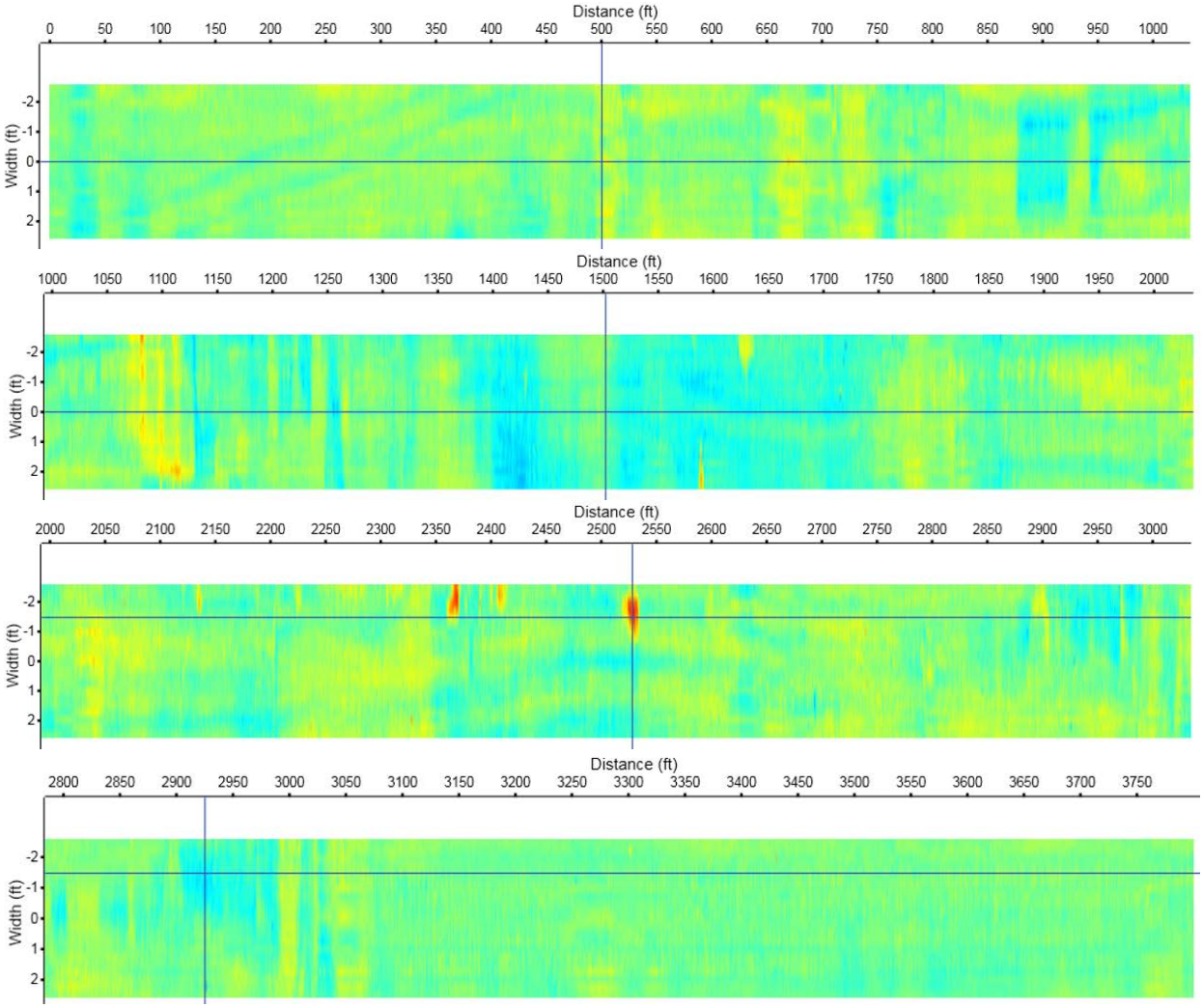

Figure 28. HMA Uniformity on SH 6, Lot 8-1 (Top of the Lift).

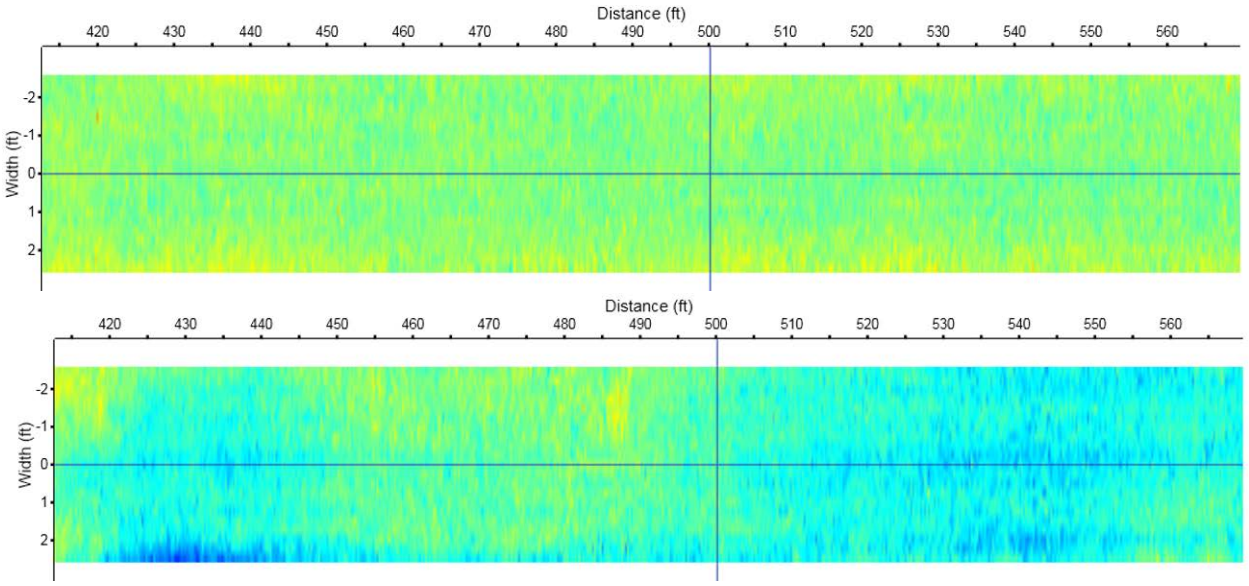

Figure 29. HMA Uniformity on SH 30: (a) Top of the Lift (0.1-in.) and (b) Bottom of the Lift (2.4-in.).

The corresponding areas measured with the RDM are shown in Figure 30 and Figure 31 for SH 6 and SH30, respectively. The average density of SH 6, Lot 8-1 was 8.5 percent with a standard deviation of about 1 percent. The average density of the Day 1, 1,000-ft test section was 6 percent with a standard deviation about 0.75 percent.

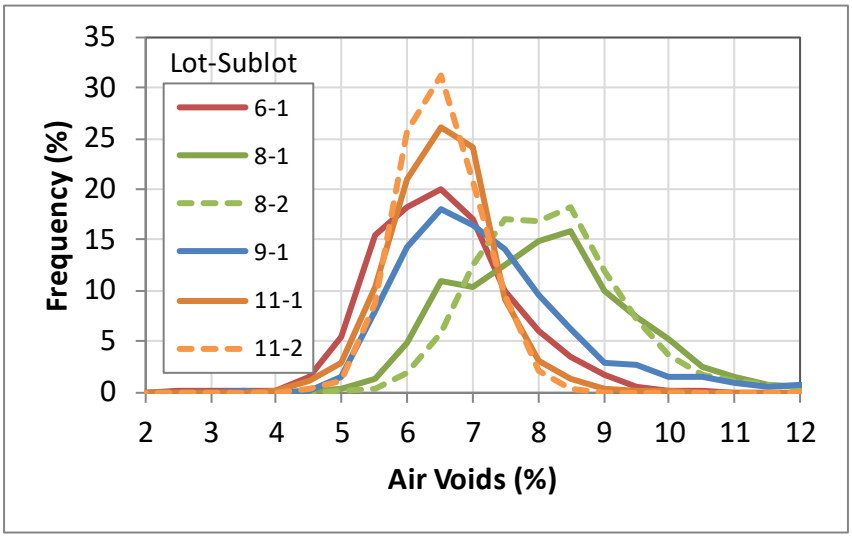

Figure 30. Predicted Void Content by Lot and Sublot-SH 6 Valley Mills-DG TyD.

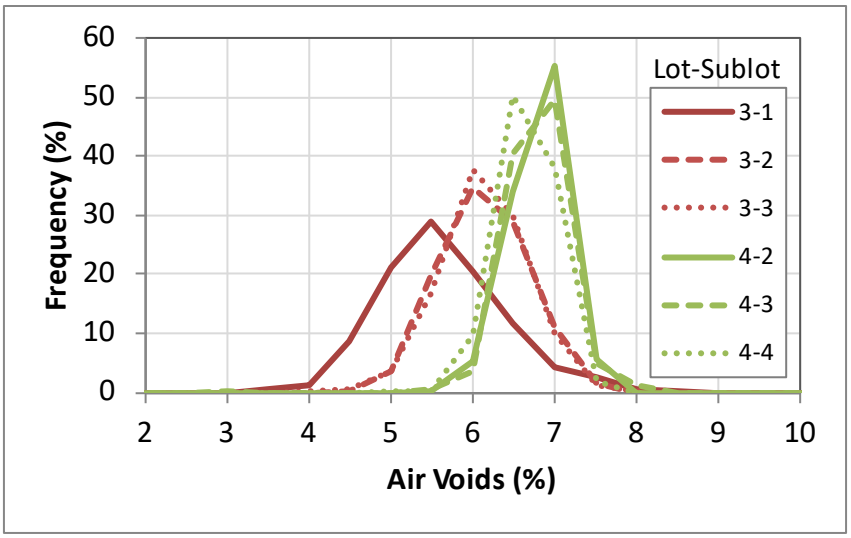

Figure 31. Predicted Void Content by Lot and Sublot-SH 30-College Station-SMA TyC.

CONCLUSION

At present, the 3D system requires further investigation for data analysis methods. Of greatest importance to this project is the ability to calculate the asphalt mixture surface dielectric. Limited work shows the system may be able to perform a density analysis function; however additional data processing techniques are required. Figure 32 illustrates how the frequency domain data can be synthesized into the time domain.

Figure 32. Example Time-Domain GPR Trace and Smoothed Trace from 3D Radar.
Note: Smoothed data shown in blue

Figure 32 illustrates:

- A time domain GPR waveform can be generated from the step frequency system. However, the resolution (red wave form) may miss the important peaks needed for calculation of dielectrics (and thus measurement of density).
- Using an interpolation to increase the resolution and smooth the data may yield a waveform more suitable for dielectric analysis (blue wave form).

Future research is required before this system could be considered as a potential candidate for use in measuring asphalt mixture density. To begin, future work should investigate the smoothing technique for generating time domain traces, determine the overall stability of this system's output over time, and evaluate the consistency of measurements across all channels.

CHAPTER 7—CONCLUSION

PROJECT SUMMARY

The rolling-density meter is a GPR-based system tailored for rapidly and continuously measuring asphalt mixture density. For a given day of paving, the RDM can make tens of thousands of measurements, a drastic improvement in testing coverage over the one or two core measurements used in current practice. This technology has the ability to supplement, and possibly eventually replace, most field coring activities, providing several advantages to stakeholders:

- Large areas can be quickly tested with minimal disruption to traffic.
- Exposure of workers in the right of way may be reduced.
- Longitudinal joint density can be evaluated for specification compliance.
- Extensive testing coverage would reduce producer and consumer risks.

The research objective was to analyze the readiness level of the RDM and provide recommendations for how this technology could be used in QC/QA. The system and methods would need to be technically sound and testing limitations clearly defined. Ideally the hardware would be robust, the software user-friendly, and the testing minimally intrusive to the current construction work flow.

To evaluate the RDM system precision, four different antennas were evaluated in a laboratory environment on six different materials. The RDM was deployed on six field projects for multiple paving days. In addition to identifying the practicality of routine implementation, researchers evaluated the reproducibility of calibration curves, precision and bias of the system and nuclear density gage, and distribution of predicted void contents. The field data were used to perform a producer and consumer risk analysis. An alternative 3D radar system was deployed on three test sections.

FINDINGS

The key findings from this research are as follows:

- Laboratory Precision Analysis:
    - In practice, averaging five scans or 500 scans to report the dielectric value does not greatly influence the mean reported surface dielectric constant.
    - Increasing the number of scans averaged did improve the precision.
    - For materials with dielectrics ranging between 4.4 and 6.4, the dielectric constant measured with the RDM should be repeatable within 0.15 or better and reproducible within 0.22 or better.
    - Antenna 7A should be investigated, as the data suggest that antenna may have imprecision and stability problems.

- Field Deployment and Data Analysis:

  - Overall air void calibrations were good with an average R^2 value of 0.76.
  - The calibration curves were unique for different paving projects (i.e., different mix designs).
  - In some cases, the curves also changed on different days of paving, which suggests there was variability in the mix produced (e.g., change in asphalt content).
  - Using different antennas did not significantly affect the overall calibration curves.
  - The RDM had negligible bias and a precision of 1 percent voids. For a given reading, the true value is expected to lie within ±2 percent voids (with 95 percent confidence).
  - The nuclear density gauge had a bias of −0.5 percent and precision of 2 percent. The true value as measured from the gauge would be within −0.5±3.8 percent voids.
  - The RDM is more precise than the nuclear density gauge and unbiased.

- Estimation of Producer and Consumer Risk:

  - Pay factors based on the RDM had some significant discrepancies from the single core pay factors, which is likely when results are based on only one sample.
  - Based on a percent within limits characterization, overall the projects had less than 2 percent below the target (over compaction), 8 percent at the target, 68 percent with an above target bonus, and over 20 percent in the above target penalty and reject category.
  - Since the RDM collects over 10,000 measurements in a given sublot, the risks to the producer (contractor) and consumer (TxDOT) are significantly reduced. The overall average air voids from density profiling may be within 0.1 percent of the true mean.

- Deployment of 3D Radar:

  - The 3D radar system produced high resolution scans of the asphalt surface and subsurface on three projects. The scans appear to be a good indication of compaction uniformity.
  - The present system was not capable of outputting surface dielectric. Custom data processing steps need to be developed and implemented into the software. Until this happens, direct comparisons with the RDM output are not possible.

RECOMMENDATIONS

Researchers recommend adopting the draft test method and equipment specifications for rapid full-coverage measurements of asphalt mixture density using GPR. See Appendix C. At this stage, the recommended methods would run parallel, not supplant, the coring requirements. The DOT should decide how exactly to incentivize districts and contractors to try the technology, such as providing bonus incentive with little or no penalties attached. The following language is suggested for incorporating into construction specifications.

General Note: Air Void Profile of Asphalt Mixtures

For Items 341, 344, and 346, the Engineer will perform an air void profile using ground-penetrating radar (GPR) to determine the portion of the sublot within the target air void content:

- Item 341: 3.8 to 8.5 percent in-place air voids
- Item 344: 3.7 to 7.5 percent in-place air voids
- Item 346: 3.7 to 7.0 percent in-place air voids

The Engineer will determine the portion of the sublot in the target air void content and a composite pay factor from the air void profile in accordance with draft Tex-XXX-F. When using air void profile, random placement sampling and testing is still applicable, and the placement pay adjustment factor is the higher of the factor from random sample locations or the composite factor from the air void profile.

Other ideas for implementation are being generated through an ongoing national effort headed by the Strategic Highway Research Program (SHRP) 2. Several states are exploring both QC and QA applications in their paving operations, such as:

- Establishing roller patterns.
- Comparing densities achieved with different mix designs.
- Identifying thermal segregation.
- Comparing inner mat and joint densities.
- Providing bonuses for longitudinal joint density.

Further research of the system and data analysis methods is also recommended. Specifically, a sensitivity analysis of mix design parameters in a laboratory environment to determine the correct thresholds to warrant a new calibration curve. Further efforts should also investigate mechanistic and mechanistic-empirical models relating the dielectric to air void content that also account for changes in the mix design. Also, experimentation and development should continue with the 3D radar system.

REFERENCES

1. Vivar, E. d. P. and J. E. Haddock. *HMA Pavement Performance and Durability.* FHWA/IN/JTRP-2005/14, Purdue University, Lafayette, IN, April 2006.

2. Wilson, B. T. and S. Sebesta. Comparison of Density Tests for Thin Hot Mix Asphalt Overlays. In *Transportation Research Record: Journal of the Transportation Research Board,* Transportation Research Board of the National Academies, Washington, D.C., January 2015, pp. 148-156.

3. Sebesta, S. and T. Scullion. *Using Infrared Imaging and Ground-Penetrating Radar to Detect Segregation in Hot-Mix Overlays.* Report 4126-1, Texas Transportation Institute, Texas A&M University System, College Station, TX, May 2002.

4. Popik, M., K. Maser, and C. Holzschuher. *Using High-Speed Ground Penetrating Radar for Evaluation of Asphalt Density Measurements.* Toronto, ON Canada, October 2009.

5. Maser, K. R. *Mapping the Density of New Asphalt Pavement with GPR*. In *BSCE News,* Boston Society of Civil Engineers, April 2014.

6. Maser, K. and A. Carmichael. *Ground Penetrating Radar Evaluation of New Pavement Density.* Report WA-RD 839.1, Inrasense, Inc, Woburn, MA, February 2015.

7. Stroup-Gardiner, M. and E. R. Brown. *Segregation in Hot-Mix Asphalt Pavements.* NCHRP Report 441, Washington, D.C., 2000.

8. *Dielectric Permittivity.* U.S. Environmental Protection Agency, Environmental Geophysics. http://www.epa.gov/esd/cmb/GeophysicsWebsite/pages/reference/properties/Electrical_Conductivity_and_Resistivity/Dielectric_Permittivity.htm. Accessed October 27, 2014.

9. Saarenketo, T. Using Ground-Penetrating Radar and Dielectric Probe Measurements in Pavement Density Quality Control. In *Transportation Research Record: Journal of the Transportation Research Board*, Washington, D.C., 1997.

10. Dai, S., K. Hoegh, and L. Khazanovich. *Asphalt Compaction Evaluation using Rolling Density Meter - MnDOT Experience*. RDM User-Group Webinar, July 20, 2017. http://www.dot.state.mn.us/mnroad/nrra/pavementconference/2017presentations/dai.ppt.

11. Silvast, M. *Air Void Content Measurement Using GPR Technology at Helsinki-Vantaa Airport, runway No. 3.* Survey Report, Roadscanners, Finland.

12. Sebesta, S., T. Scullion, and T. Saarenketo. *Using Infrared and High-Speed Ground-Penetrating Radar for Uniformity Measurements on New HMA Layers.* SHPR 2 Report S2-R06C-RR-1, Transportation Research Board of the National Academies, Washington, D.C., 2013.

13. Al-Qadi, I. L. Using Microwave Measurements to Detect Moisture in Asphaltic Concrete. *Journal of Testing and Evaluation*, Vol. 20, No. 1, 1992, pp. 43-50.

14. Al-Qadi, I. L., Z. Leng, and A. Larkin. *In-Place Hot Mix Asphalt Density Estimation Using Ground Penetrating Radar*. ICT Report No. 11-096, University of Illinois at Urbana-Champaign, December 2011.

15. Zhao, S., P. Shangguan, and I. L. Al-Qadi. Application of Regularized Deconvolution Technique for Predicting Pavement Thin Layer Thicknesses from Ground Penetrating Radar Data. *NDT&E International*, Vol. 73, Department of Civil and Environmental Engineering, University of Illinois at Urbana-Champaign, Urbana-Champaign, July 2015.

16. Lytton, R. L. *System Identification and Analysis of Subsurface Radar Signals*, T.A.M. University, Editor 1995, Licensed to Lyric Technologies, Inc: Houston, TX, USA.

17. Lytton, R. L. Characterizing Asphalt Pavements for Performance. In *Transportation Research Record: Journal of the Transportation Research Board, No. 1*, Washington, D.C., 2000, pp. 5-16.

18. John, E., S. Sebesta, B. Hewes, H. Sahin, R. Luo, J. Button, R. L. Lytton, C. Herrera, R. Hatcher, and F. Gu. *Development of a Specification for Flexible Base Construction.* FHWA/TX-13/0-6621-2, Texas Transportation Institute, College Station, TX, August 2013.

APPENDIX A: FIELD DATA

US 183-TOM Data

Day	Location	Cores		GPR Spot					Water Flow (min.)	Nuclear Gauge
		6-in., full-depth		#3	#4	#7	All			
		Bulk SG	Est Bulk Voids	Avg	Avg	Avg	Avg	StDev		
1	1-1	2.192	6.5	4.82	4.75	4.84	4.80	0.04	282.1	140.1
	1-2	2.215	5.6	5.01	4.91	5.04	4.98	0.06	282.1	142.0
	1-3	2.231	4.9	5.01	4.88	5.03	4.97	0.07	282.1	143.9
	1-4	2.241	4.4	5.12	4.98	5.12	5.07	0.06	55.9	144.8
	1-5	2.162	7.8	4.64	4.51	4.63	4.59	0.06	55.9	139.2
	1-6	1.990	15.1	4.02	3.99	4.07	4.03	0.03	3.3	126.7
	1-7	2.071	11.7	4.41	4.33	4.41	4.38	0.04	13.5	133.6
	1-8	1.978	15.7	4.04	4.02	4.09	4.05	0.03	1.6	123.8
	1-9	1.994	15.0	4.22	4.21	4.27	4.23	0.03	3.0	127.3
	1-10	1.928	17.8	3.83	3.82	3.90	3.85	0.04	1.4	123.4
2	2-1	2.080	11.3		4.41				7.4	132.9
	2-2	2.096	10.6		4.57				13.5	133.6
	2-3	2.136	8.9		4.61				27.6	133.4
	2-4	2.102	10.3		4.60				27.6	134.5
	2-5	2.135	9.0		4.66				55.9	135.0
	2-6	2.095	10.7		4.61				13.5	135.7
	2-7	2.106	10.2		4.55				282.1	135.6
	2-8	2.034	13.3		4.34				5.4	130.7
	2-9	2.168	7.6		4.76				55.9	142.9
	2-10	1.950	16.8		4.12				1.9	128.4
3	3-1	2.062	12.1		4.43					129.3
	3-2	2.161	7.8		4.70					137.3
	3-3	2.103	10.3		4.56					133.9
	3-4	2.082	11.2		4.60					134.2
	3-5	2.067	11.9		4.55					130.6
	3-6	2.054	12.4		4.44					130.6
	3-7	2.005	14.5		4.31					126.4
	3-8	2.088	10.9		4.45					134.9
	3-9	2.007	14.4		4.21					125.6
	3-10	2.082	11.2		4.57					132.7

US 90-Ty D Data

Day	Location	Cores		GPR Spot		Nuclear Gauge
		6-in., full-depth		#4		
		Bulk SG	Est Bulk Voids	Avg	StDev	
1	1-1	2.369	3.0	5.67	0.17	149.0
	1-2	2.328	4.7	5.52	0.18	145.5
	1-3	2.356	3.6	5.53	0.19	144.5
	1-4	2.355	3.6	5.68	0.19	150.8
	1-5	2.327	4.7	5.60	0.19	146.8
	1-6	2.349	3.8	5.64	0.19	148.0
	1-7	2.264	7.3	5.36	0.17	139.9
	1-8	2.265	7.3	5.21	0.16	140.2
	1-9	2.283	6.6	5.34	0.18	143.4
	1-10	2.344	4.0	5.62	0.16	148.3
2	2-1	2.277	6.8	5.50	0.18	143.5
	2-2	2.295	6.1	5.42	0.18	145.5
	2-3	2.171	11.1	4.97	0.21	134.0
	2-4	2.284	6.5	5.20	0.17	140.4
	2-5	2.208	9.6	5.08	0.16	139.1
	2-6	2.194	10.2	5.06	0.19	134.9
	2-7	2.167	11.3	4.83	0.16	132.6
	2-8	2.263	7.4	5.16	0.16	140.2
	2-9	2.294	6.1	5.46	0.19	143.6
	2-10	2.256	7.7	5.34	0.25	140.7
3	3-1	2.251	7.8	5.42	0.17	141.2
	3-2	2.198	10.0	5.22	0.17	140.8
	3-3	2.235	8.5	5.20	0.17	139.1
	3-4	2.254	7.7	5.39	0.18	140.5
	3-5	2.237	8.4	5.22	0.17	136.4
	3-6	2.221	9.1	5.17	0.17	138.0
	3-7	2.241	8.3	5.32	0.17	138.8
	3-8	2.238	8.4	5.32	0.16	138.8
	3-9	2.306	5.6	5.41	0.17	142.6
	3-10	2.223	9.0	5.20	0.16	138.3

IH 10-Ty C Data

Day	Location1	Cores		GPR Spot					Nuclear Gauge
		6-in., full-depth					Overall		
		Bulk SG	Est Bulk Voids	#3	#4	#7	Avg	StDev	
1	1-1	2.249	7.7	5.45	5.45	5.52	5.48	0.03	136.9
	1-2	2.326	4.5	6.18	6.23	6.33	6.25	0.06	143.3
	1-3	2.285	6.2	5.78	5.80	5.85	5.81	0.03	143.5
	1-4	2.369	2.7	6.01	6.03	6.16	6.07	0.07	145.4
	1-5	2.371	2.7	5.99	6.08	6.14	6.07	0.06	135.9
	1-6	2.237	8.2	5.62	5.67	5.67	5.65	0.02	137.6
	1-7	2.216	9.0	5.40	5.46	5.46	5.44	0.03	139.5
	1-8	2.258	7.3	5.62	5.64	5.72	5.66	0.04	138.3
	1-9	2.351	3.5	6.13	6.22	6.28	6.21	0.06	143.2
	1-10	2.277	6.5	5.55	5.59	5.59	5.58	0.02	142.4
2	2-1	2.268	7.0	5.43	5.42	5.43	5.43	0.00	143.0
	2-2	2.305	5.4	5.75	5.71	5.69	5.72	0.02	143.1
	2-3	2.293	6.0	5.71	5.66	5.73	5.70	0.03	141.0
	2-4	2.249	7.8	5.34	5.27	5.29	5.30	0.03	135.5
	2-5	2.225	8.8	5.38	5.36	5.37	5.37	0.01	136.9
	2-6	2.283	6.4	5.55	5.53	5.59	5.56	0.03	132.2
	2-7	2.281	6.4	5.69	5.68	5.70	5.69	0.01	141.1
	2-8	2.293	5.9	5.59	5.56	5.59	5.58	0.01	140.7
	2-9	2.277	6.6	5.63	5.60	5.66	5.63	0.02	155.0
	2-10	2.268	7.0	5.61	5.53	5.55	5.56	0.04	150.4
3	3-1	2.235	8.1	6.20	5.79	5.52	5.84	0.28	139.1
	3-2	2.280	6.3	7.05	6.67	5.96	6.56	0.45	141.3
	3-3	2.295	5.7	6.18	6.23	5.91	6.11	0.14	142.9
	3-4	2.281	6.2	5.79	5.69	5.66	5.71	0.05	139.8
	3-5	2.281	6.2	5.80	5.73	5.72	5.75	0.04	145.5
	3-6	2.308	5.2	6.07	5.93	5.96	5.98	0.06	141.0
	3-7	2.260	7.1	5.78	5.70	5.74	5.74	0.03	141.7
	3-8	2.246	7.7	5.70	5.62	5.64	5.65	0.04	137.6
	3-9	2.277	6.4	5.72	5.65	5.66	5.67	0.03	142.8
	3-10	2.246	7.7	5.70	5.71	5.58	5.66	0.06	138.3

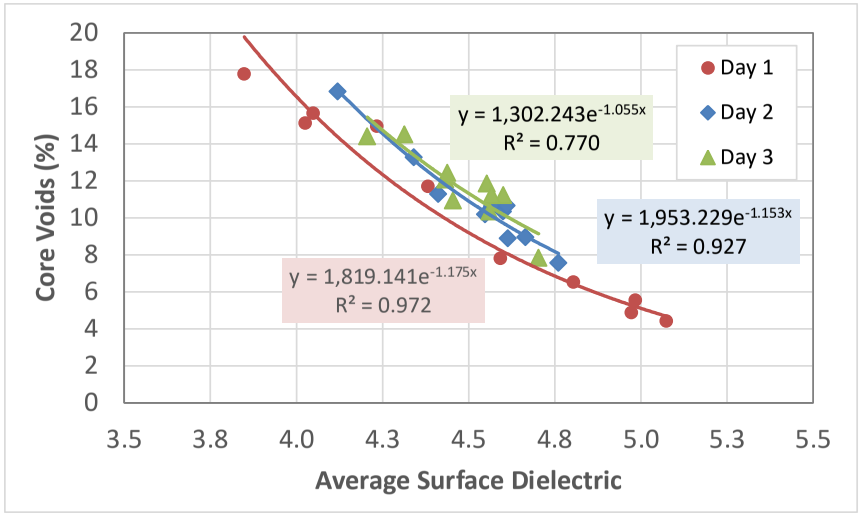

(a)

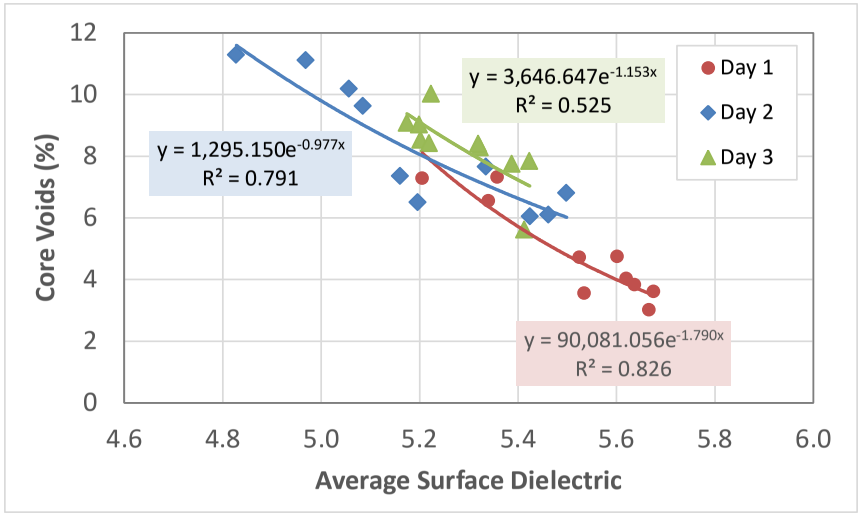

(b)

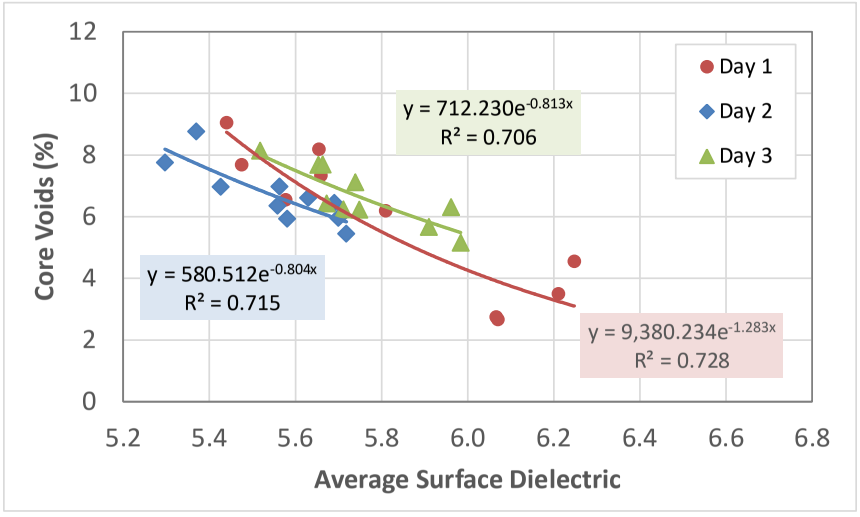

(c)

Calibration of Surface Dielectric to Core Voids: (a) US 183-TOM-F, (b) US 90-SP Ty D, and (c) IH 10-SP Ty C.

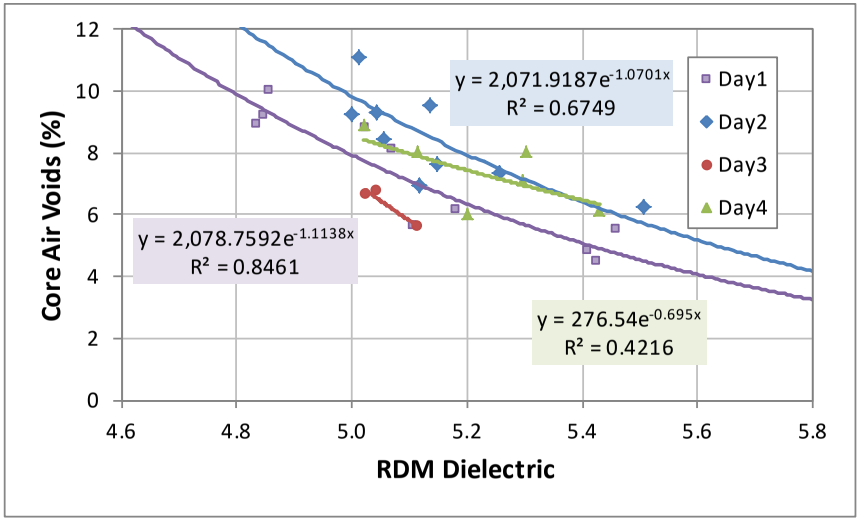

Calibrations (SH 6-Valley Mills).

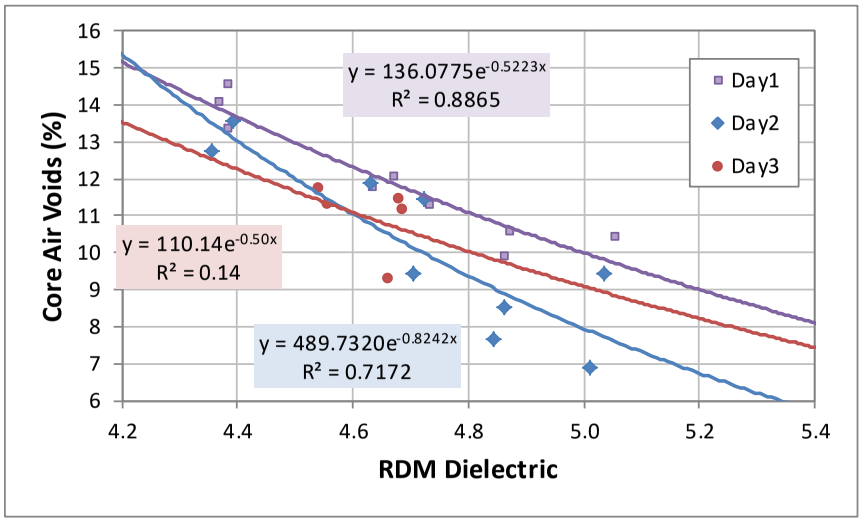

Calibrations (SH 6-Lake Waco).

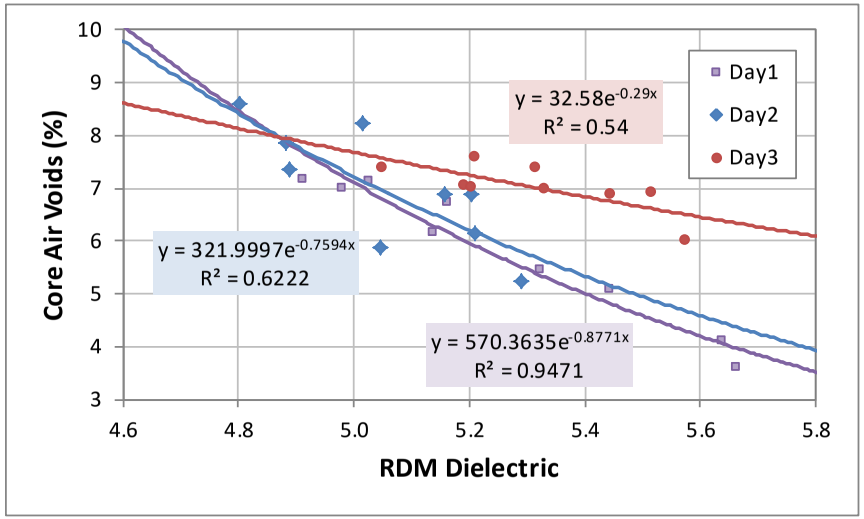

Calibration of Surface Dielectric to Core Voids: (a) SH 6-Valley Mills-DG Ty D, (b) SH 6-Waco-TOM Ty C, and (c) SH 30-SMA Ty C.

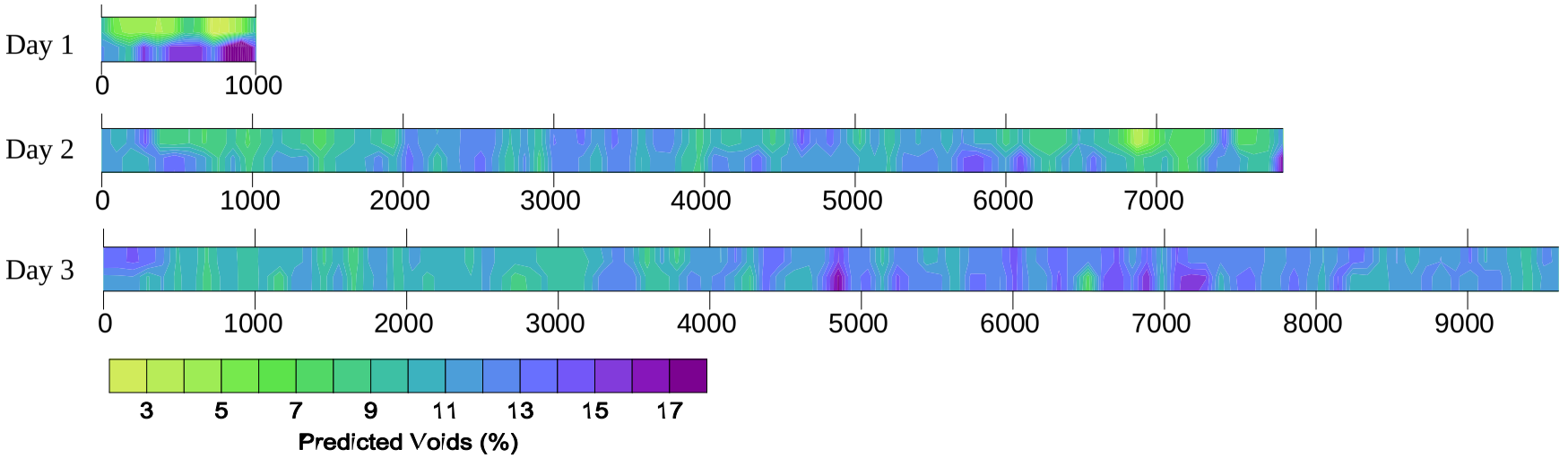

Predicted Voids (US 183-TOM).

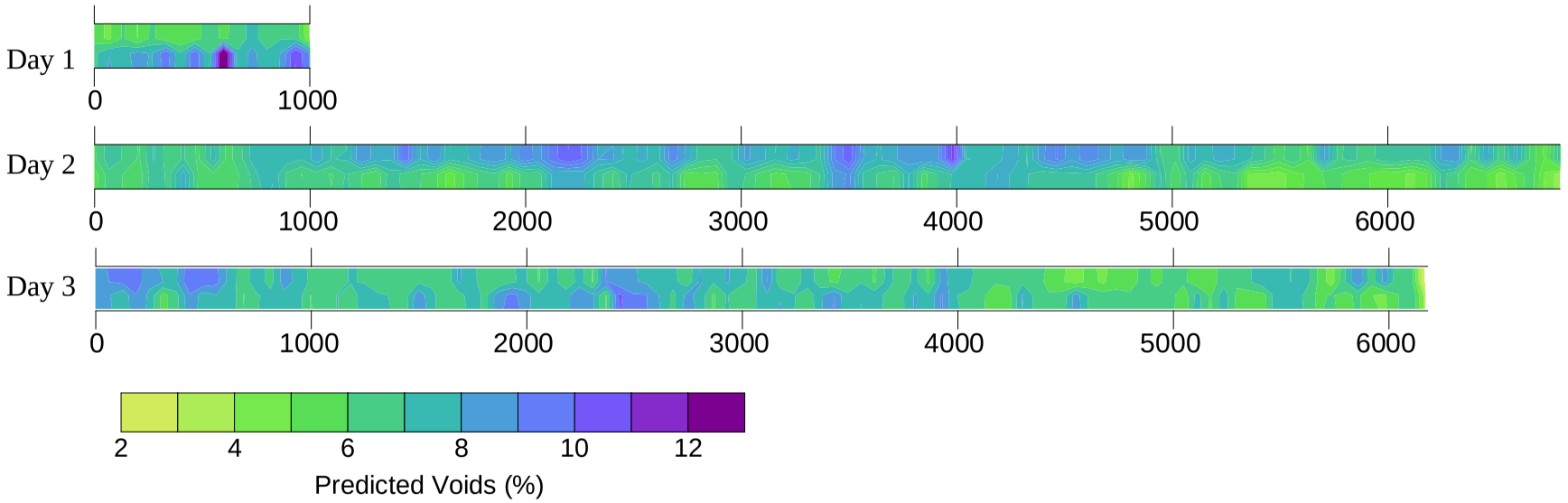

Predicted Voids (US 90-Ty D).

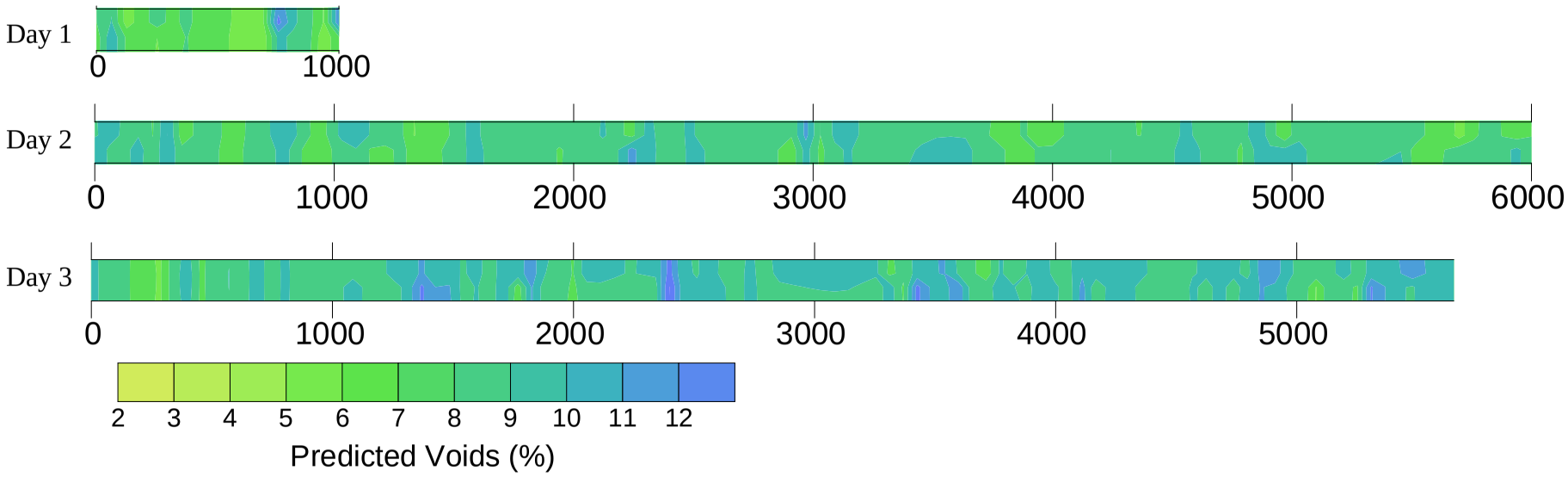

Predicted Voids (IH 10-Ty C).

APPENDIX B: PROCESSING AND STATISTICAL ANALYSIS DETAILS

PROCESS FOR RANKING DIELETRIC RANKINGS

The following is a discussion on the process of assigning the dielectric rankings of high, moderate, and low.

The official calibration process was only performed on the first day of production for each project. What this entailed was measuring a 1,000 ft section with the RDM, then using the core locator algorithm within the software to identify potential high, moderate, and low dielectric locations. In practice, an operator would then take two samples from each of these groups for a total of six cores. In our study, on production days where cores locations were selected randomly (Days 2 and 3), this predictive ranking by the software was never performed.

To establish calibration curves, researchers had to assign rankings to the cores and choose two from each group. This process was more complex than simply assigning the rank based on the final measured dielectric value. In practice, the core locator algorithm only *suggests* which locations would fit a particular rank, whereas the actual dielectric when returning to the recommended location can often fall into a different rank. For example, one location ranked as high should have a dielectric of 5.6, but when returning to that location, the highest reading the researchers might obtain is 5.1, and is actually lower than a location ranked as moderate.

To account for this issue, researchers identified a linear regression between the software-estimated dielectric values and actual spot dielectric values for the three days with calibration curves. The mean error (bias) and standard deviation of the error (precision) of the residuals was calculated. The remaining dielectric data were then run through the same linear regression and then the error term was randomly assigned according to the equation below. The new hypothesized estimated dielectrics were ranked numerically. The three highest were assigned to high, the next four to moderate, and the last three to low.

$$Est.Diel = NormInv(Rand, Mean, StDev)$$

Where *Est. Diel* = Hypothetical estimated dielectric.
NormInv = Inverse of the normal distribution given parameter inputs.
Rand = Random number between 0 and 1.
Mean = Mean of the error, in this case 0.
StDev = Standard deviation of the residual.

STATISTICAL EQUATIONS

$$Precision_{Avg} = \frac{\sum_i^{1000} StDev_i}{1000}$$ Equation B-1

Where $Precision_{Avg}$ = Overall precision of the RDM, %.
$StDev_i$ = Standard deviation of the residual errors for the sample, %.
i = ith random sample of calibration and validation cores.

$$Bias_{Avg} = \frac{\sum_i^{1000} Bias_i}{1000}$$ Equation B-2

Where $Bias_{Avg}$ = Overall bias of the RDM, %.
$Bias_i$ = Bias of a given random sample, %.
i = ith random sample of calibration and validation cores.

$$Voids = 100 - \frac{Density}{62.4\ pcf} * 100$$ Equation B-3

where *Voids* = Core air void content, %.
Density = Compacted unit weight from a nuclear density gauge, pcf.

$$Precision = \sqrt{\frac{\sum(voidsPred_i - voidsActual_i)^2}{n-1}}$$ Equation B-4

Where *Precision* = Precision of the nuclear density gauge, %.
$voidsPred_i$ = Predicted voids for a given sample, %.
$voidsActual_i$ = Actual void content of the core, %.
i = ith pair of samples.
n = Number of paired samples.

$$Bias = \frac{\sum(voidsPred_i - voidsActual_i)}{n}$$ Equation B-5

Where *Bias* = Bias of the nuclear density gauge, %.
$voidsPred_i$ = Predicted voids for a given sample, %.
$voidsActual_i$ = Actual void content of the core, %.
i = ith pair of samples.
n = Number of paired samples.

Reproducibility of Calibration Curves by Antenna

Linear regression model:

logVoids ~1 + proj_day + diel +antenna+proj_day*diel

Variable	Ty III SumSq	DF	MeanSq	F	pValue
proj_day	1.059	11	0.096	6.858	2.79E-10
diel	3.321	1	3.321	236.630	1.61E-39
antenna	0.033	2	0.016	1.172	0.311
proj_day:diel	1.035	11	0.094	6.701	5.12E-10
Error	4.099	292	0.014		

Estimated Coefficients:	Estimate	SE	tStat	pValue
(Intercept)	8.7116	0.4311	20.208	2.06E-57
proj_day_IH10_2	-2.3133	0.96398	-2.3998	0.0170
proj_day_SH30-College Station_1	-2.7410	0.61257	-4.4746	0.0000
proj_day_SH30-College Station_2	-3.4021	0.80523	-4.2251	0.0000
proj_day_SH30-College Station_3	-5.3712	0.82712	-6.4939	0.0000
proj_day_SH6-Lake Waco_1	-3.8099	0.62716	-6.0748	0.0000
proj_day_SH6-Lake Waco_2	-2.6060	0.637	-4.0911	0.0001
proj_day_SH6-Lake Waco_3	-4.2579	2.0975	-2.0299	0.0433
proj_day_SH6-Valley Mills_1	-1.2656	0.63917	-1.9801	0.0486
proj_day_SH6-Valley Mills_2	-1.6597	0.8033	-2.0661	0.0397
proj_day_SH6-Valley Mills_4	-3.7476	1.0886	-3.4425	0.0007
proj_day_US183_1	-1.7859	0.48751	-3.6633	0.0003
diel	-1.2008	0.074004	-16.2260	0.0000
antenna_2	-0.0156	0.016356	-0.9511	0.3424
antenna_3	0.0094	0.016425	0.5706	0.5687
proj_day_IH10_2:diel	0.3851	0.17193	2.2398	0.0259
proj_day_SH30-College Station_1:diel	0.3956	0.11101	3.5637	0.0004
proj_day_SH30-College Station_2:diel	0.5338	0.15341	3.4798	0.0006
proj_day_SH30-College Station_3:diel	0.9391	0.15196	6.1796	0.0000
proj_day_SH6-Lake Waco_1:diel	0.6815	0.12244	5.5657	0.0000
proj_day_SH6-Lake Waco_2:diel	0.3957	0.12359	3.2015	0.0015
proj_day_SH6-Lake Waco_3:diel	0.7560	4.50E-01	1.6800	0.0940
proj_day_SH6-Valley Mills_1:diel	0.1252	0.1181	1.0602	0.2899
proj_day_SH6-Valley Mills_2:diel	0.2453	0.15157	1.6183	0.1067
proj_day_SH6-Valley Mills_4:diel	0.6319	0.20495	3.0832	0.0022
proj_day_US183_1:diel	0.1841	0.089483	2.0572	0.0406

Number of observations: 318, Error degrees of freedom: 292

Root Mean Squared Error: 0.118

R-squared: 0.895, Adjusted R-Squared 0.886

F-statistic vs. constant model: 99.9, p-value = 1.94e-127

Reproducibility of Calibration Curves by Day of Production

Linear regression model:
logVoids ~ 1 + diel*proj + diel*day

Variable	Ty III SumSq	DF	MeanSq	F	pValue
diel	5.1253	1	5.1253	287.7	3.78E-36
proj	0.59793	5	0.11959	6.7127	0.00001
day	0.096721	2	0.048361	2.7146	0.06962
diel:proj	0.64543	5	0.12909	7.246	4.43E-06
diel:day	0.15528	2	0.077642	4.3583	0.01453
Error	2.5653	144	0.017815		

Estimated Coefficients:	Estimate	SE	tStat	pValue
(Intercept)	5.7246	0.56167	10.192	7.29E-19
diel	-0.70507	0.098097	-7.1875	2.89E-11
	0			
proj_'SH30-College Station'	0.048736	0.84119	0.057937	9.54E-01
proj_'SH6-Lake Waco'	-0.14173	0.8621	-0.1644	0.86964
proj_'SH6-Valley Mills'	1.4966	0.90665	1.6506	0.1009
proj_'US183'	1.5053	0.70829	2.1252	0.035206
proj_'US90'	3.2691	0.88245	3.7045	0.000297
	0			
day_'2'	-0.12816	0.32302	-0.39675	0.69211
day_'3'	-0.96638	0.28174	-3.4301	7.80E-04
	0			
diel:proj_'SH30-College Station'	-0.06909	0.15585	-0.44332	0.65817
diel:proj_'SH6-Lake Waco'	0.009395	0.17056	0.055082	0.95615
diel:proj_'SH6-Valley Mills'	-0.31956	0.16932	-1.8873	0.061053
diel:proj_'US183'	-0.37711	0.13791	-2.7344	0.007003
diel:proj_'US90'	-0.63148	0.16101	-3.922	0.000133
	0			
diel:day_'2'	0.041909	0.063858	0.65628	0.51265
diel:day_'3'	0.23046	0.054501	4.2285	4.07E-05

Number of observations: 166, Error degrees of freedom: 150
Root Mean Squared Error: 0.143
R-squared: 0.856, Adjusted R-Squared 0.841
F-statistic vs. constant model: 59.3, p-value = 3.6e-55

APPENDIX C: TEST METHOD, EQUIPMENT SPECIFICATIONS, AND CONSTRUCTION IMPLEMENTATION

This appendix contains the following:

- DRAFT Test Method for Density Profile of Asphalt Mixtures Using Ground Penetrating Radar (Tex-XXX-X)
- Equipment specifications for an asphalt dielectric profiling system (DPS). This is based heavily on a draft American Association of State Highway and Transportation Officials specification developed during SHRP2 project R06C: Rapid Technologies to Enhance Quality Control on Asphalt Pavements.
- Revisions to construction specifications to implement the draft test method.

DRAFT Test Method for

Density Profile of Asphalt Mixtures Using Ground Penetrating Radar

TxDOT Designation: Tex-XXX-X

Draft Date: December 2017

1. SCOPE

1.1 Use this test method to obtain a density profile of an asphalt paving project using ground penetrating radar (GPR).

1.2 This method includes procedures for general system calibration, calibration of the GPR to the specific asphalt mixture, data collection, analysis procedures, and report summary.

2. APPARATUS

2.1 *Ground penetrating radar system* — A GPR system, comprised of antennas, signal processors, vehicle or cart mounting hardware, and software, capable of the following:

2.1.1 Collecting single or multiple-channel GPR data using air-coupled antennas with central operating frequency between 1 and 3 GHz. The antennas must meet the performance specifications of Table 1.

Table 1— Performance summary table with required limits.

Measure Description	Required Limit
Short Term Dielectric Stability	Max: 0.06
Long Term Dielectric Stability	Max: 0.08
Antenna Dielectric Variation*	Max: 0.08

*Multichannel systems only

2.1.2 Recording positon using GPS with an accuracy of ±15 ft or better and using a distance measuring instrument with a minimum operational tolerance of 0.25 ft/mile.

2.1.3 Measuring the surface dielectric constant in real time and recording the data at fixed longitudinal distance intervals as small as 0.5 ft at walking speeds and every 2 ft at driving speeds.

2.1.4 Providing software that:

Displays readings in real time using a line graph or heat map format.
Calculates recommended calibration core locations.
Calculates summary data and creates reports according to Section 5 of this method.

NOTE — Further details for the GPR system and requirements are contained in Appendix C of TxDOT Research Report 0-6889-1: Evaluation of the Rolling Density Meter for Rapid Continuous Measurement of Asphalt Mixture Density.

3. PROCEDURE

3.1 *System Calibration* – Before collecting data, allow the GPR to warm up and then calibrate each antenna in the system with an air and metal plate calibration according to the manufacturer's recommendations.

3.2 Air Void Calibration:

3.2.1 Each unique mix design requires an air void calibration.

NOTE — The calibration originating from another mix design is not valid. A new calibration may also be warranted with significant changes to the job mix formula (greater that ±0.3 percent change in asphalt content, or change in aggregate source).

3.2.2 Under traffic control, collect a GPR profile on newly placed asphalt at least 1,000-ft long with a multichannel system, or 2,000-ft long with a single-channel system. Measurements must recorded every 0.5 ft at a speed no faster than 10 mph. For multichannel systems, the antennas should be spaced at least 1-ft apart and at least 12 in. from the mat edge.

3.2.3 Identify nine calibration locations comprised of three high-, three moderate-, and three low-dielectric values. Note the dielectric and station # of each location.

NOTE —The difference between the highest and lowest average dielectric should be 0.75 or greater. Further guidance on how to select calibration

locations is given in Appendix C of TxDOT Research Report 0-6889-1 - Evaluation of the Rolling Density Meter for Rapid Continuous Measurement of Asphalt Mixture Density.

3.2.4 Return to each location and use the live dielectric measurement in time-mode to precisely find a location with a similar value as previously measured. Mark the location with minimal contamination to the surface (i.e., use paint marker or marking crayon).

NOTE — No data are actually recorded in this step.

3.2.5 With one designated antenna, perform a measurement directly over the marked location, moving the antenna ±2 to 3 in. to cover the diameter of a core sample (FIGURE 1). Record the average dielectric.

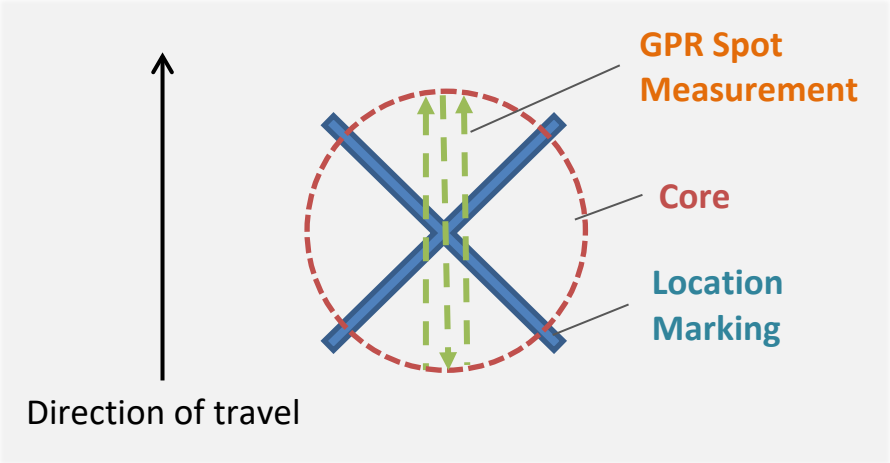

FIGURE 1 – Configuration for Spot Measurement.

3.2.6 Obtain cores directly over each marked location.

NOTE — The center of the core must be within ±1.5 in. of the center of the marking.

3.2.7 Measure the bulk specific gravity and air void content of each core according to Tex-207-F Part I or Part VI and Tex-227-F.

3.2.8 Plot the dielectrics *(x-axis) vs* voids (y-axis) data and calculate the calibration parameters *a* and *b* for the following non-linear (power) regression equation.

$$Voids = a * Diel^{b}$$ **Equation (1)**

3.3 Data Collection:

3.3.1 Position the antenna/s over the desired profile line/s as shown in FIGURE 2. Options include:

Left half of the mat.
Right half of the mat.
Center of the mat where the rollers overlap.
The confined joint (3–5 in. within the joint).

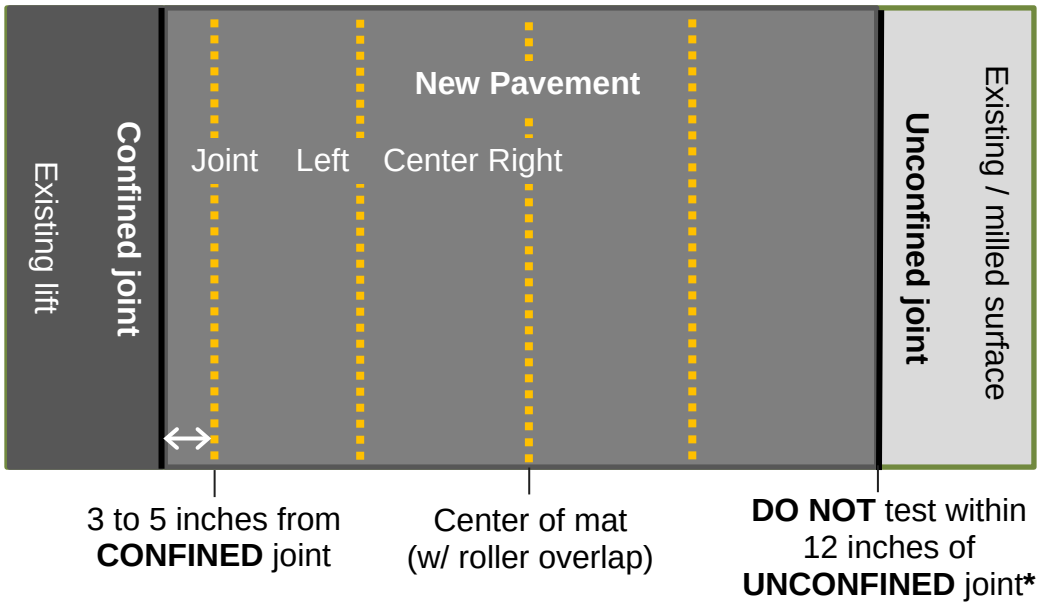

FIGURE 2 – Profiles Recommended for Testing.

NOTE — Do not test within 12 in. of the unconfined joint before the adjoining lift is constructed. The pavement edge drop-off will interfere with the GPR signal. After the adjoining lift is placed, the joint can be tested with a profile 3–5 in. from the joint.

NOTE — Mounted green lasers may be used as a guide to maintain a consistent lateral position. This is especially important for joint profiles.

3.3.2 Provide appropriate project and location details as prompted by the GPR software.

3.3.3 Collect the desired profile length of data in distance-mode at the speed and data density recommended by the GPR manufacturer.

3.3.4 Note any surface anomalies during the profile (i.e., surface water from rollers, metal bridge joints, bridge decks, utility covers)

4. CALCULATIONS

4.1 Perform the following using the GPR software.

4.1.1 Query data for the desired analysis length, typically corresponding to one sublot.

4.1.2 Compute the air void contents from the dielectric data based on Equation 1.

4.1.3 Process the data with a 10-ft moving average filter.

4.1.4 Calculate a histogram of the overall air void contents for profiles within the mat. A separate histogram shall be calculated for joint profiles.

4.1.5 Calculate the 5th percentile, 50th percentile (median), and 95th percentile air void contents for each histogram.

5. REPORT

5.1 Table of Summary Data:

5.1.1 Populate a table with the following data.

50th percentile (median) void content.
Percent within limits for each void content rating. Subdivide the ratings for above and below the in-place air voids compaction required for the mix type.
Composite pay factor.
90th percentile pay factor (average of the 5th and 95th percentile factors).

5.2 Table of Reject Areas:

5.2.1 Provide a table of stations and mean air void contents that are designated as Reject. This table should only consider **data within the mat** and not the joint data. Report only locations 50 ft or longer with the Reject assignment, or locations 100 ft or longer with at least 50 percent of the length assigned as Reject.

5.2.2 As applicable, provide a table of stations and mean air void contents for **joints** designated as Reject. Detail exactly which joint is indicated. Report only locations 50 ft or longer with the Reject assignment, or locations 100 ft or longer with at least 50 percent of the length assigned as Reject.

5.3 Heat Maps of Air Void Contents:

5.3.1 Provide a heat map of air void contents (10-ft moving average) for the desired analysis length or station limits using the GPR software filter (e.g., FIGURE 3).

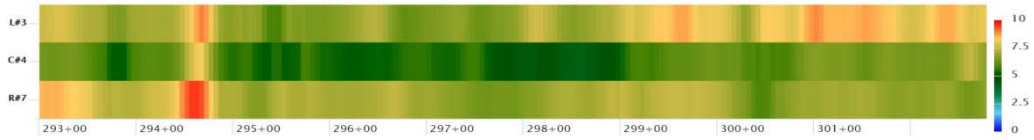

FIGURE 3 – Heat Map.

NOTE — The maps may present the discrete profile data or present the data after smoothing and surface contouring techniques.

5.3.2 Color scale the heat map based on the project's pay schedule. Include a legend with the map:

Full bonus = green.
Bonus = yellow-green.
Penalty = yellow.
Reject = red.
Hatching, or similar markings, should be used to distinguish between air void contents above and below the target.

SPECIFICATIONS FOR AN ASPHALT DENSITY PROFILING SYSTEM

SCOPE

This standard specifies the equipment and software requirements for a DPS. Calibration and verification procedures are also detailed.

A DPS uses GPR technology to continuously measure asphalt compaction quality up to freeway speeds. The system reports the asphalt surface dielectric, which is strongly correlated to asphalt air void content (FHWA/TX-92/1233-1). As dielectric increases, air void content decreases.

A DPS may be a single- or multichannel system and may be cart- or vehicle-mounted.

HARDWARE REQUIREMENTS

Dielectric Profiler System Overview

The DPS consists of the following components.

- Vehicle or Cart.
    - Antenna boom.
    - Distance measuring instrument (DMI).
    - Global positioning system (GPS).
- Single or multichannel air coupled GPR system (see ASTM D4748).
    - Radar antenna/s.
    - Sampler/recorder.
    - Signal processing system.
- Computer and software.
- Metal plate and validation block.

The system shall measure the dielectric constant of the surface based on the GPR surface reflection. The system shall be capable of recording these data at both fixed distance intervals (distance mode) and at fixed time intervals (time mode).

Vehicle or Cart

A vehicle or cart shall be provided to carry the GPR system, computer, metal plate, and be equipped with a DMI and GPS receiver.

Antenna boom – Non-metallic boom to maintain the antenna/s at a fixed vertical height at least 24 in. away from any large metal body such as the vehicle frame. Processing algorithms should account for vertical movement from the vehicle suspension. When vehicle mounted, the system shall be structurally capable of traveling up to 50 mph with

tolerable antenna movement. For multichannel systems, the antennas should be positioned in the center of the lane and in the wheel paths. Optionally, each antenna's lateral position may be adjustable.

DMI – The vehicle or cart should be instrumented with a DMI with a minimum operational tolerance of 0.25 ft/mile.

GPS – The vehicle or cart should be instrumented with a GPS with a minimum operational tolerance of ±15 ft. Higher accuracy is warranted for forensic work.

Air Coupled GPR

Single or multichannel air-coupled GPR system with an operational frequency of between 1 and 3 GHz shall be used. All antennas shall have the same frequency.

Performance Specifications: The GPS system shall pass the performance specifications in Table 1. These are based on the metal plate reflection tests recommended by the Texas A&M Transportation Institute with the Federal Highway Administration, FHWA/TX-92/1233-1 for general purpose GPR. Each of these measurements shall be determined prior to the first use of the equipment.

Table 1— Performance summary table with required limits.

Measure Description	Required Limit
Short Term Dielectric Stability	Max: 0.06
Long Term Dielectric Stability	Max: 0.08
*Antenna Dielectric Variation**	Max: 0.08

**Multichannel systems only*

Short Term Dielectric Stability – Stability of the measured dielectric constant over a short time period. In time-mode, collect 50 surface dielectric measurements over a validation block at a minimum rate of 15 scans per second. Stacking or moving average techniques may be used if the DPS has the capability of collecting data at a faster rate. Calculate the short term stability according to Equation C-1:

$$STDS = eSTmax - eSTmin \qquad \text{Equation C-1}$$

where:

eSTmax = maximum recorded dielectric over 50 scans.
eSTmin = minimum recorded dielectric over 50 scans.

Long Term Dielectric Stability – Stability of the measured dielectric constant over an extended period of time. In time-mode, collect dielectric measurements over a validation block for 1 hour continuously at a minimum rate of 15 scans per second. Stacking or moving average techniques may be used if the DPS has the capability of collecting data at a faster rate. Calculate the long term stability according to Equation C-2:

$$LDS = eLmax - eLmin$$ Equation C-2

where:
eLmax = maximum recorded dielectric over 20 minute time period.
eLmin = minimum recorded dielectric over 20 minute time period.

Antenna Dielectric Variation – Variation among the dielectric measurements from the different DPS antennas. Applicable to multichannel DPS systems only. In time-mode, collect 1,000 dielectric measurements with each antenna over a validation block. Calculate the mean value from each antenna. Calculate the antenna variation using Equation C-4.

$$Antenna\ Dielectric\ Variation = eAmax - eAmin$$ Equation C-4

where:
eAmax = maximum mean dielectric among all DPS antennas.
eAmin = minimum mean dielectric among all DPS antennas.

Metal Plate and Validation Block

Metal Plate – A stainless steel metal plate, a minimum of 18 × 18 in. square and 0.125 in. thick, shall be used for calibration and performance validation of the GPR antennas.

Validation Block – A block of plastic insulating material shall be used for performance validation of the GPR antennas. The block shall conform to ASTM D2520 and ASTM D150-11. The block shall have a known dielectric value between 2.5 and 6. The minimum block size shall be 18 × 18 in. and 2 in. thick.

SOFTWARE REQUIREMENTS

Data Collection

Meta Data – As a minimum, the software shall store the following meta-data:

- Date-time.
- Project name.

Dielectric Data

Calibration – Before every data collection period, the software shall prompt the user to perform an air and metal plate calibration process for each antenna, as directed by the manufacturer.

Dielectric – The software shall calculate the surface dielectric constant from the surface reflection using Equation C-5. Recording individual trace data is not necessary.

$$\sqrt{\varepsilon_p} = \frac{1-\frac{A_p}{A_m}}{1+\frac{A_p}{A_m}}$$ Equation C-5

where:
ε_p = Dielectric value of the pavement surface.
A_p = Reflection amplitude from the pavement surface.
A_m = Source amplitude, as estimated with a metal plate reflection measurement.

Air Void Conversion – The software may provide an empirical conversion from dielectric constant to asphalt air void content using a linear, logarithmic, or power equation.

Distance-mode – The software shall be capable of recording dielectric data at fixed distance intervals as small as every 0.5 in. *The reported value may be the result of moving average, stacking, and/or oversampling techniques.*

Time-mode – The software shall be capable of recording dielectric data at fixed time frequency.

Signal Correction – The software shall account for potential cell tower interference. This may be done through oversampling, stacking, and/or averaging the data.

Distance – DMI and GPS measurements shall accompany each dielectric measurement.

***Data Display* – The DPS software shall:**

Display the data in real-time.

Display the current dielectric values from each antenna, with an appropriate moving average filter. Typically, 10 ft average is reasonable.

Provide a plot of dielectric vs. distance or time. The plot shall be a heat map and/or line graph. The scale for the dielectric axis should cover a range of 1.5, typically from 4 to 6.5. The scale should adjust to center around the data without changing the scale range. Minimize changes to the scale as much as possible so as to avoid confusion and misinterpretation of data.

***Data Analysis* —The DPS software shall perform the following data analyses on-site:**

- Data filtering by:
- Centerline offset.
- Stationing.
- Antenna serial #.
- Summary statistics (applied to any combination of data filtering).
- Average dielectric.
- Median dielectric.
- Standard deviation of dielectric.
- Dielectric value at nth percentile (user specified percentage).
- Percent below/within/above limits (user specified dielectric range).
- Percent below limit (at user specified dielectric value).
- Joint ratio (mean dielectric along the joint divided by mean dielectric along the center of the mat).
- Summary visuals (applied to any combination of data filtering).
- Plot of dielectric vs. distance. The plot shall be a heat map and/or line graph.
- Histogram of the data.

CONSTRUCTION SPECIFICATION REVISIONS

For initial implementation, researchers recommend an approach that provides incentive to use the air void profile. The basic approach recommended at this time is:

- Continue performing cores at random sample locations for each placement sublot.
- When using air void profile, perform one profile per sublot, and determine a composite pay adjustment factor for each sublot.
- When using air void profile, the placement pay adjustment factor is the higher of the factor from random sample locations or the composite factor from the air void profile.

To begin establishing use of air void profile in construction specifications, researchers recommend a general note.

General Note: Air Void Profile of Asphalt Mixtures
For Items 341, 344, and 346, the Engineer will perform an air void profile using GPR to determine the portion of the sublot within the target air void content:

- Item 341: 3.8 to 8.5 percent in-place air voids.
- Item 344: 3.7 to 7.5 percent in-place air voids.
- Item 346: 3.7 to 7.0 percent in-place air voids.

The Engineer will determine the portion of the sublot in the target air void content and a composite pay factor from the air void profile in accordance with draft Tex-XXX-F. When using air void profile, random placement sampling and testing is still applicable, and the placement pay adjustment factor is the higher of the factor from random sample locations or the composite factor from the air void profile.